

Master Thesis
TVVR 16/5003

Siltation Problems at the Landeyjahöfn Harbour, Iceland

Governing Processes
and Coastal Evolution

Samuel Brudfors
Peter Pantzar



Division of Water Resources Engineering
Department of Building and Environmental Technology
Lund University

Siltation Problems at the Laneyjahöfn Harbour, Iceland

Governing Processes
and Coastal Evolution

By:
Samuel Brudfors
Peter Pantzar

Master Thesis
Division of Water Resources Engineering
Department of Building & Environmental Technology
Lund University
Box 118
221 00 Lund, Sweden

Water Resources Engineering
TVVR-16/5003
ISSN 1101-9824

Lund 2016
www.tvrl.lth.se

Master Thesis
Division of Water Resources Engineering
Department of Building & Environmental Technology
Lund University

Swedish title: Sedimentationsproblem i hamnen Landeyjahöfn, Island
English title: Siltation Problems at the Landeyjahöfn Harbour,
Iceland
Authors: Samuel Brudfors
Peter Pantzar
Supervisor: Magnus Larson
Examiner: Hans Hanson
Language: English
Year: 2016
Keywords: Longshore Sediment Transport; Coastal Evolution;
Landeyjahöfn; Siltation; Bar Evolution; EBED; Qtrans;
Cascade

Acknowledgements

First of all we would like to thank our supervisor Professor Magnus Larson at the division of Water Resources Engineering, Faculty of Engineering, Lund University, for all the help and support with our master thesis. We would also like to thank Sigurdur Sigurdarson and the Icelandic Road and Coastal Administration for giving us a warm welcome in Iceland with an interesting field study and for funding our trip to Iceland. Furthermore, all the data and interesting discussion provided by the Icelandic colleagues are appreciated, which made this Master Thesis possible.

Abstract

The Landeyjahöfn Harbour, located on the south coast of Iceland, has since its opening in 2010 been suffering from siltation problems. Sediment deposited in the harbour entrance, preventing the ferry to run at full capacity. The problem was addressed in previous studies, but without arriving at a sustainable solution, stimulating the present study with the overall objective to investigate the sediment transport, coastal evolution, and the influence on the harbour. Wave data, measurements of bathymetries, shorelines, and beach profiles were used in the analysis to provide sufficient information for reaching a solution that improves the conditions at the harbour. The wave transformation model EBED, together with a 58-year long time series of input wave data, was used to simulate the nearshore wave climate. The resulting nearshore waves were further used as input to the longshore sediment transport model Qtrans and the regional shoreline evolution model Cascade. The model simulations showed that the location of the harbour is in an area with a complex transport pattern. Accumulation is likely to occur in this area, which would be one reason for sedimentation inside the harbour. Placing long groins or jetties that reach past the bar could be a solution to decrease the longshore sediment transport at the harbour. However, further investigations are warranted to find the most appropriate solutions to improve the conditions at the harbour.

Sammanfattning

Hamnen i Landeyjahöfn, som är belägen på Islands sydkust, har sedan öppning 2010 lidit av sedimentationsproblem. Sediment ackumuleras i hamninloppet, vilket förhindrar färjan från att användas med full kapacitet. Problemet har tagits upp i tidigare studier, men utan att nå en hållbar lösning. Dessa studier initierade föreliggande studie med syfte att undersöka sedimenttransport, kustutveckling samt påverkan på hamnen för att försöka nå en lösning som förbättrar förhållandena vid hamnen. Vågdata, mätning av batymetrier, strandlinjer och strandprofiler har använts för att analysera förutsättningarna vid hamnen. Vågutbredningsmodellen EBED användes för att simulera det kustnära vågklimatet med utgångspunkt från en 58-år lång serie av vågdata på djupt vatten. Det strandnära vågklimatet som erhöles användes senare som underlag för den kustparallella sedimenttransportmodellen Qtrans och strandlinjeutvecklingsmodellen Cascade. Modellerna visar att området kring hamnen är komplext och ackumulation sannolikt förekommer, vilket kan vara en anledning till sedimentationen i hamnen. Placering av långa hövder/pirar som sträcker sig förbi reveln kan vara en lösning för att minska den kustparallella sedimenttransporten vid hamnen. Det behövs dock ytterligare undersökningar för att utvärdera de möjliga lösningarna.

Table of contents

1	Introduction	1
1.1	Background.....	1
1.2	Objectives	1
1.3	Procedure	1
1.4	Report Outline	2
2	Littoral Transport	4
2.1	Cross-shore Sediment Transport	4
2.2	Longshore Sediment Transport	6
3	Study Area.....	9
3.1	General Overview.....	9
3.2	Wave and Water Level Conditions.....	11
3.3	Geology and Geomorphology	11
3.4	Sediment Transport.....	13
4	Landeyjahöfn Harbour	15
4.1	Landeyjahöfn Harbour.....	15
4.2	Siltation Problems.....	17
4.3	Previous Studies	17
4.3.1	Morphological Evolution	18
4.3.2	Wave Climate.....	19
4.3.3	Sediment Transport	20
4.3.4	Evaluation of Radical Solutions.....	22
5	Data Compilation and Analysis.....	27
5.1	Bathymetric Data	27
5.2	Wave Data	27
5.3	Morphological Evolution.....	29

5.3.1	Morphometric Changes of Shoreline	29
5.3.2	Bar Evolution	30
6	Nearshore Wave Transformation	33
6.1	Governing Equations	33
6.2	Model Input and Implementation	34
6.2.1	Bathymetric Data.....	34
6.2.2	Wave Data	35
6.2.3	EBED Output Locations.....	36
6.3	Simulation Results	37
6.3.1	Wave Pattern EBED	37
6.3.2	Location Results	41
6.4	Validation of Wave Model	44
6.4.1	Extension of the Wave Model Grid.....	45
6.4.2	Input Boundaries and Wave Energy.....	48
6.4.3	Cell Size	50
7	Longshore Sediment Transport - Qtrans	51
7.1	Governing Equations	51
7.2	Model Input and Implementation	51
7.3	Calibration of Transport Coefficient	53
7.3.1	Methodology	53
7.3.2	Results	54
7.3.3	Concluding Remarks	55
7.4	Results	56
7.4.1	Sediment.....	56
7.4.2	Net Sediment Transport	57
7.4.3	Gross Sediment Transport.....	58
7.5	Analysis of Results	59
7.5.1	Net Sediment Transport	59

7.5.2	Gross Sediment Transport.....	60
7.5.3	Comparison Between Qtrans and DHI's Litpack.....	61
8	Long-term Coastal Evolution – Cascade.....	65
8.1	Governing Equations	65
8.2	Model Input and Implementation	66
8.3	Calibration Cascade	67
8.4	Simulation Results	68
9	Analysis of Bar Evolution	71
9.1	Comparison of Bathymetries and Sediment Transport.....	71
9.2	Bar Evolution and Comparison	76
10	Analysis of Possible Solutions	79
10.1	Groins.....	79
10.2	Reservoirs	81
11	Discussion	83
11.1	Sediment Transport Modelling	83
11.2	Morphological Evaluation	84
11.3	Possible Solutions	84
12	Conclusions	87
13	Further Investigations.....	89
14	References	91
15	Appendix	95
15.1	Shoreline Difference	95
15.2	Wave Rose for Bar Evolution.....	98
15.3	Bar Volume Variation.....	103

1 Introduction

1.1 Background

The Landeyjahöfn harbour has since its opening in 2010 been suffering from siltation problems, where sediment is being deposited in the harbour entrance, preventing the ferry that runs between Landeyjahöfn and the Vestmannaeyjar (Westman Islands) from operating safely. The harbour is located on the south coast of Iceland, which experiences a large longshore sediment transport because of the exposed conditions to waves and currents. Extensive investigations were conducted before the construction of the harbour, including field data collection and numerical modelling. However, due to the complexity of the situation at Landeyjahöfn, siltation problems occurred in the harbour in spite of the special design made to bypass the sediment transported alongshore. After the problems appeared, additional investigations were carried out, particularly frequent, detailed surveys of the bathymetry around the harbour. In spite of the studies performed, problems with siltation in the harbour entrance remain. The governing processes controlling the sediment transport and deposition have not been clearly established and remedial measures to alleviate the situation are still needed.

1.2 Objectives

The overall objectives of this study are to investigate the basic processes governing the sediment transport and coastal evolution at Landeyjahöfn, as well as the influence of the harbour on the transport pattern and sediment deposition around the harbour. In addition, different possible solutions to reduce the deposition of sediment in the harbour area are considered. These solutions are evaluated, qualitatively and quantitatively, to assess the effects of the selected different measures to reduce the deposition of sediment in the harbour area with focus on improving the navigational conditions. Finally, possible trends in the variation of the longshore bar properties are investigated.

1.3 Procedure

A survey of relevant previous studies, covering coastal processes in general, the environmental conditions at the site, and the investigations from the Landeyjahöfn project, was performed. Existing background data, especially wave data and bathymetric data, were compiled, reviewed, and analysed for a

general understanding of the conditions at the site. This analysis formed the basis for establishing the governing sediment transport processes and their characteristics. The extensive bathymetric data collected earlier by Siglingastofnun (the Icelandic Maritime Administration) and nowadays by Vegagerðin (Icelandic Road and Coastal Administration) have not been analysed in detail and related to the wave conditions; thus, it was expected that these data would yield a wealth of information on the governing processes at the site. Numerical modelling of the sediment transport and coastal evolution, primarily at a longer time scale, was undertaken to develop a description of the typical regional sediment transport pattern and its temporal and spatial variation. After a better understanding of the governing processes at the site and the sediment transport characteristics, selected measures for improving the navigational conditions by reducing and/or changing the sediment deposition around the harbour were investigated. In order to quantify the effects of such measures, coastal evolution modelling was carried out, primarily looking at the construction of groins or jetties to prevent siltation in the harbour.

1.4 Report Outline

The report contains the following main chapters, with the specified content:

Chapter 1: *Introduction* – Background, objectives and procedure of the thesis are given.

Chapter 2: *Littoral Transport* – Littoral transport, in general, and cross-shore and longshore sediment transport, in particular, is discussed.

Chapter 3: *Study Area* – The study area and the influence of the Westman Islands and the river Markarfljót is described. Also, wave climate, tidal variations, geology, geomorphology, and sediment transport on the south coast of Iceland is reviewed.

Chapter 4: *Landeyjahöfn Harbour* – The properties of the harbour in and the sedimentation problems are summarized. The previous studies made by DHI are presented.

Chapter 5: *Data Compilation and Analysis* – The bathymetric data and the wave climate used in the models as well as the observed shoreline change and bar evolution are discussed.

Chapter 6: *Nearshore Wave Transformation* – The nearshore wave transformation model EBED, the inputs and implementation, and the results from the simulations made are presented. Model validation is also performed.

Chapter 7: *Longshore Sediment Transport from Qtrans* – The longshore sediment transport model Qtrans, the inputs and implementation, and the results are discussed. A calibration of the transport coefficient is made to adjust the calculated sediment transport along the coastline to agree with observations of shoreline change.

Chapter 8: *Long-term Coastal Evolution from Cascade* – The numerical model Cascade that simulates the regional sediment transport and coastal evolution is employed. Inputs, implementation, and results are described, including the procedure to calibrate the transport coefficient.

Chapter 9: *Bar Evolution Analysis* – An analysis of the bar evolution is made by comparing the bathymetries and the sediment transport calculated with Qtrans. The bar volume taken from profile measurements and calculated by Cascade are compared to evaluate the performance of the model.

Chapter 10: *Analysis of Possible Solutions* – Possible solutions to remediate the harbour sedimentation is presented. The main solution analysed consists of a groin/jetty preventing sediment to reach the harbour, but excavation to create reservoirs for sediment deposition is also reviewed.

Chapter 11: *Discussion* – The results from the sediment transport modelling are discussed. An evaluation of the bar evolution and the possible solutions is also included.

Chapter 12: *Conclusions* – The conclusions of the thesis are presented.

Chapter 13: *Further Investigation* – Further investigations are suggested.

2 Littoral Transport

Sediment transport in a coastal area is important to investigate when analysing the conditions for man-made activities and structures in the area. Littoral transport is defined as the movement of sediment in the nearshore zone by waves and currents. This nearshore zone is known as the littoral zone, encompassing the zone between the backshore and the most seaward location where breaking waves influence the transport. Littoral transport is typically divided into two transport modes: longshore sediment transport (LST) and cross-shore sediment transport (transport directed along and perpendicular to the coastline, respectively). Both these modes depend on the waves that propagate towards the beach and the currents that the waves induce. The currents are directed both in the longshore and cross-shore direction, although the former tend to be much stronger and more important for the transport. The transport in the swash, which is when the waves wash up water on the subaerial portion of the beach, is sometimes considered to be a third mode of transport, see Figure 2 (Hanson, 2015). The effects from swash, including uprush and backwash, are that it moves sediment up and down the foreshore, contributing to both the cross-shore and longshore sediment transport.

At the micro scale, there are three different mechanisms that transport sediment: bed load, suspended load, and sheet flow. Bed load is when grains move along the bottom in contact, induced by shear from the water moving above the sediment bed. Suspended load is the transport of grains by currents after the grains have been lifted from the bed by shear and turbulence. Sheet flow occurs when the grains move collectively as a layer along the bottom caused by large shear stresses. (Hanson, 2015)

2.1 Cross-shore Sediment Transport

Cross-shore sediment transport is the sediment transport perpendicular to the shoreline by the combined effects of waves and currents acting on the beach. Cross-shore sediment transport is primarily determined by the steepness of the waves, the sediment grain size, and the beach slope. In general, high steep waves move finer material offshore and low waves of long period move coarser material onshore (U.S. Army Corps of Engineers, 1984). Steep waves are more common in winter than summer and therefore a difference can be observed in the beach profile shape for these two periods. The beach profile

in summer has a larger volume sediment on the beach compared to the profile in winter, which can be observed in Figure 1. The morphodynamics of the beach profile are protecting the beach face against the rougher wave climate in winter or during storm events, since sediment is moving offshore to create a larger bar that reduces the wave energy at the beach face (Hanson, 2015). If the amount of sediment transported onshore at a certain location is equal to the amount transported offshore a dynamic equilibrium is obtained with no depth change.

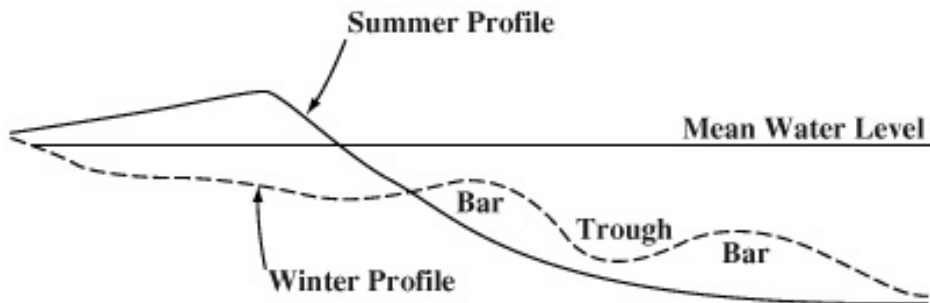


Figure 1: Cross-shore transport. The figure illustrate how seasonal changes in wave climate affect the beach profile. During winter storms, the dry beach is eroded and seaward cross-shore sediment transport results in the formation of one or more offshore bars. Under the milder wave climates of summer, the sediment returns to the dry beach, building up a distinct berm. (Seymour, 2005)

2.2 Longshore Sediment Transport

Longshore sediment transport (LST) refers to sediment movement parallel to the shoreline. LST occurs when approaching waves break and stir up sediment, simultaneously as an alongshore current is generated due to the incident wave angle to the shoreline, see Figure 2.

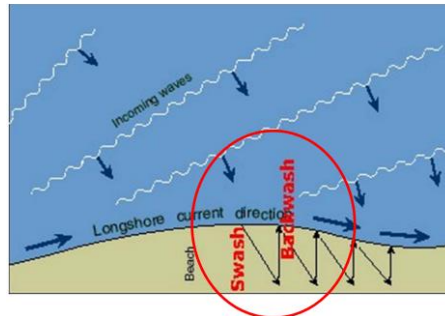


Figure 2: An alongshore current is generated from the incoming waves breaking at an angle to the shoreline. (Hanson, 2015)

The LST, being dependent on the alongshore wave energy flux, is strongly affected by the breaking angle of the approaching waves to the shoreline, which is illustrated in Figure 3 and explained in the points below. (Grunnet & Kristensen, 2013)

- Waves that approach perpendicular towards the shoreline (wave angle $\alpha = 0$ deg) do not generate LST.
- Waves that are approaching almost parallel to the shoreline generate low LST due to the strong refraction that reduces the incoming wave height and therefore the breaking wave height.
- The maximum LST is obtained when the waves approach at a 45-degree angle to the shoreline.

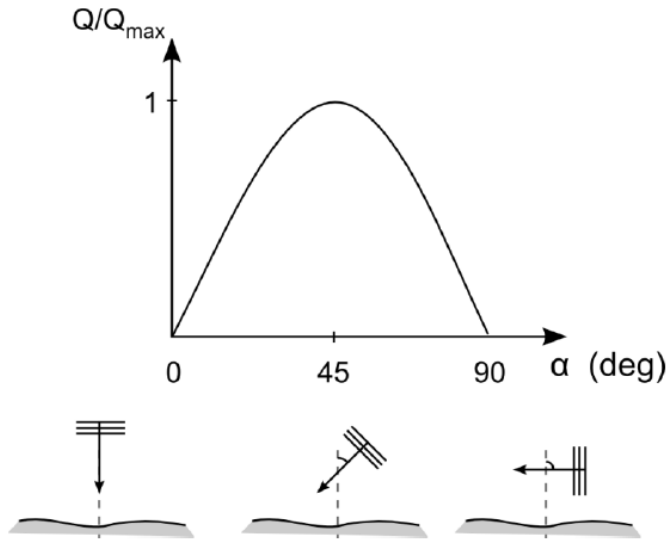


Figure 3: The variation of the longshore sediment transport as a function of the wave angle towards the shoreline. The notations in the bottom illustrate the orientation of the approaching waves. (Grunnet & Kristensen, 2013)

Because of the variability in the incident waves, the longshore transport direction typically varies at a short time scale, in accordance with the wave climate. (U.S. Army Corps of Engineers, 1984) If the LST rate is larger out from a specific area compared to the LST rate in, the shoreline will erode since sediment is removed from the area. For a stable stretch of shoreline the LST rates in and out both will be equal and therefore no significant change in shoreline position will occur since no sediment has left the system.

The gross LST rate is the total amount of sediment transported passed a specific section perpendicular to the shoreline, irrespective of the transport direction (that is, the absolute sum of the rates). In contrast, the net LST rate refers to the amount taking into account the transport direction. The net LST rate is important when studying the long-term effects that a marine structure can have on the sediment pattern, for example, determining the accumulation rate and shoreline advance updrift a structure. However, if dredging of an inlet or a navigational channel is a concern, the gross LST rate is of interest.

3 Study Area

3.1 General Overview

The harbour Landeyjahöfn is located in Bakkafjara on the south of Iceland, see Figure 4. South of the harbour are the Westman Islands located which also can be observed in the figure. It is between these two places that the ferry is operating. The nearshore conditions at Landeyjahöfn vary significantly, where the wave climate consists of waves travelling both from southwest and southeast, producing marked LST along the coast.



Figure 4: The left picture shows the location of Landeyjahöfn on the south coast of Iceland, whereas the right picture displays a detail of the harbour where the Westman Islands can be observed south of the harbour.

The Westman Islands provides shelter for the harbour from waves propagating from the south, which has led to a salient build up behind the islands. During normal conditions a longshore bar is present in the vicinity of the harbour that reduces the incoming wave energy. The combination of the effects of the shelter provided by the islands, the presence of the longshore bar, and a low net LST rate were the reasons why the harbour was placed at its present location. (Grunnet & Kristensen, 2013)

Located east of the harbour is the river Markarfljót, which has a large watershed area (Jónsdóttir, 2006). The main source for the river is meltwater from the glaciers Eyjafjallajökull and Mýrdalsjökull and it runs out into the Atlantic Ocean east of Landeyjahöfn, supplying the shoreline with sediment. In April 2010 the volcano Eyjafjallajökull erupted, which led to a large supply of sand and gravel to the delta east of the harbour. This supply significantly affected the sediment balance of the area and even today it is believed to influence the conditions at the harbour (Sigurdarson, 2016). The

river mouth has also historically shown to be shifting cyclically along the coast over the years, which has been a major problem for the area where the harbour is located, see Figure 5.

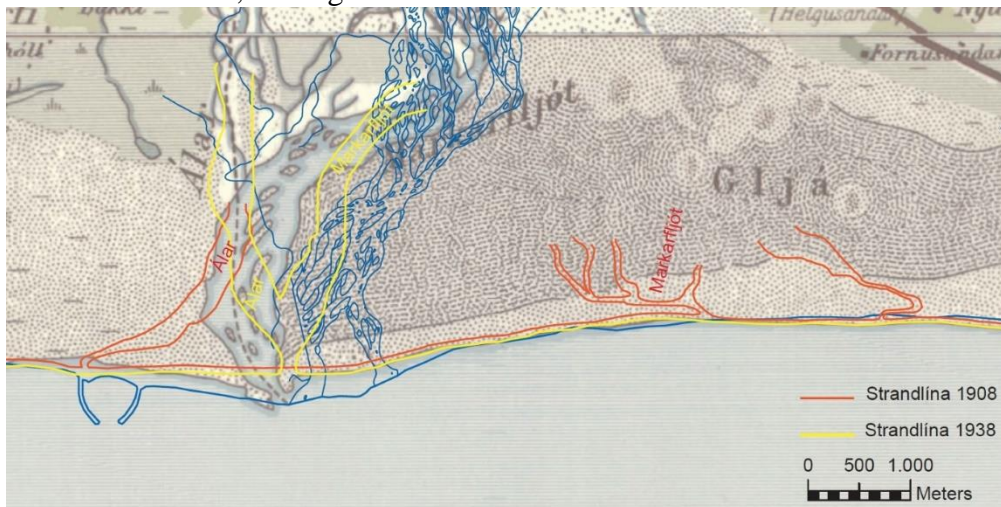


Figure 5: The movement of the river Markarfljót near the coast between 1908 and 1938.

Therefore, after the harbour was built, a long wall was constructed close to the harbour to divert the outlet of the river to a more eastern location, see Figure 6. This structure was also introduced to affect the LST at the coast by trying to force the sediment to the east.



Figure 6: The wall constructed close to the harbour to divert the outlet of the river Markarfljót to a more eastern location.

In 2010, the same year as the eruption of Eyjafjallajökull, the wave conditions changed, so that instead of the waves consistently producing LST to the east, the waves changed direction and started mainly to produce LST to the west. This west-going LST combined with the extreme large supply of sand from Markarfljót led to a build-up of shallow areas around the harbour. Within a couple of years, however, these shallow areas rapidly deepened again. (Grunnet & Kristensen, 2013)

3.2 Wave and Water Level Conditions

The wave climate outside the coast of Landeyjahöfn varies a lot over the year. During the winter months October to March larger significant wave heights occur compared to the summer months June to August. From 2013 and forward the wave conditions have mainly been dominated by waves from southwest and southeast. The areas further to the west of the harbour are more exposed to large waves. Due to the shelter provided from the Westman Islands the areas closer to the harbour are less exposed to large waves, thus having a milder wave climate. The rough wave climate with high waves during the winter months results in large LST. (Grunnet & Kristensen, 2013)

The water level outside Landeyjahöfn is affected by tidal variation. The tides at Landeyjahöfn are semidiurnal and mesotidal, meaning that there are two highs and two lows during a tidal day (25 hours) with variation of 2-4 meters. The neap tidal range is 1.2 m and the spring tidal range 2.8 m.

The effect of the tidal flows on the sediment transport (longshore and cross-shore) is typically small since the velocity is small in shallow water. The water level variation may have some effects on a short time scale, since it determines the level from which the wave can influence the sea bottom and dry part of the beach; but over longer periods this effect is in general not significant. This study will focus on the long-term sediment transport effects and therefore the tidal variation will not be included in the analysis. However, when looking at extreme events it could be necessary to evaluate the impact of the tide.

3.3 Geology and Geomorphology

The coastal stretch is morphologically characterized by a sandy barrier extending in a southeast (SE) to south (S) directions. The sandy barrier consists of basalt grain sand, where the grain size varies from 0.2-0.5 mm

depending if they are located seawards or landwards the bar. The density of the sand in the area has shown to be $2,850 \text{ kg/m}^3$ (Sigurdarson, 2016).

Within the nearshore zone a longshore bar is located about 800 m offshore at roughly a depth of 5.5 m. The bar varies over the year due to seasonal variation of the wave climate, which affects the sediment transport and therefore the bar. An interesting object, is a gap in the bar, located outside the entrance of the harbour. The data of the bathymetry shows that the gap has been present for a long time, which indicates that the gap is natural and stable over time, see Figure 7. The reason for why the gap occurs has not been determined. However, the gap was a reason to build the harbour at its location, since the ferry would be able to enter the port by navigating through the natural gap. (Hjelmager Jensen, et al., 2007)



Figure 7: In front of the harbour entrance a gap in the bar can be observed where the waves are not breaking.

The variation of the shoreline evolution from 1954 to 2000 varies significant from west to east of the harbour. West of the harbour the shoreline has been stable over the years compared to the east, where a variability of 300 m seawards has occurred over the years (Elfrink, et al., 2006). The shoreline between Bakkafjara and Thorlakshöfn is rather straight with a small curve towards Thorlakshöfn, which also indicates that the shoreline is rather stable (TVRL, 2005).

3.4 Sediment Transport

The sediment transport around Landeyjahöfn is dominated by the wave conditions. The waves outside the coast of Landeyjahöfn and south coast of Iceland are large and therefore large wave energy is propagated towards the coastline that result into large sediment transport travelling longshore the coast at Landeyjahöfn. The supply of sediment from Markarfljót as mentioned in 3.1 has an impact on the sediment transport at Landeyjahöfn since more sediment is deposited into the coastal system. The sediment transport occurs at the bar, harbour and at the shoreline. (Grunnet & Kristensen, 2013).

4 Landeyjahöfn Harbour

Before Landeyjahöfn was built the ferry running from Thorlakshöfn to the Westman Islands was the way to reach the islands, see Figure 8 for location of Thorlakshöfn. The travelling time of the ferry is 2 hours and 45 minutes and it runs only a few times per day. In order to reduce the travelling time and achieve a better connection between the mainland and the islands, Landeyjahöfn Harbour was built in 2010. The travelling time was reduced to 30 minutes with more departures per day to a lower price. Therefore, the harbour made it easier for people living on the islands to reach the mainland, but also for tourists to visit the islands. (Sigurdarson, 2016) However, because of the siltation problem, the harbour has not functioned as planned and therefore full capacity has not been achieved.

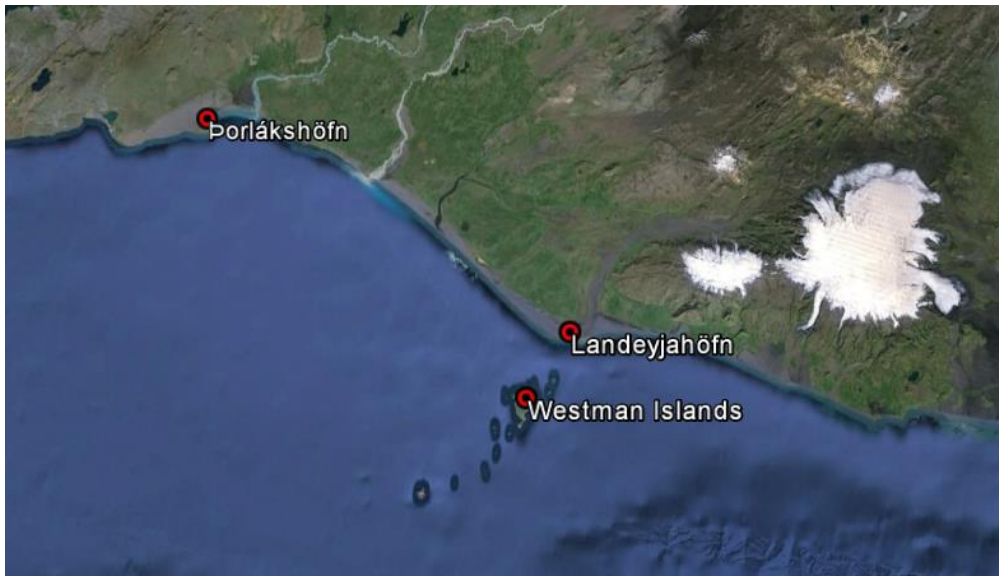


Figure 8: Locations of Thorlakshöfn, Landeyjahöfn and Westman Islands. (GoogleEarth, 2016)

4.1 Landeyjahöfn Harbour

The harbour was constructed with a width of about 600 meters having two breakwaters that stretch out 550 meters from the coast with a 75° angle, see Figure 9.



Figure 9: Landeyjahöfn Harbour. (Bogi, 2014)

The design was chosen to obtain a bypassing effect for the large amount of sediment transported seaward of Landeyjahöfn Harbour. The bypassing effect is achieved by the streamlined layout of the harbour, so that sediment can move passed the entrance without being entrained into the harbour. This design has been employed in several locations in Denmark; Hanstholm harbour is one example, located 80 km north of Thorsminde, see Figure 10. This harbour was built at a critical location where the net sediment transport is about 0.4 million m³/year northward and the gross transport about 1.5 million m³/year (Grunnet & Kristensen, 2013). However, at Landeyjahöfn Harbour the bypassing effect has not been functioning as intended, but large accumulation has occurred at the entrance as discussed in the following section.



Figure 10: Hanstholm Harbour in Denmark (Elfrink, et al., 2006).

4.2 Siltation Problems

Since the opening of the Landeyjahöfn Harbour there has been problems with the navigation depth in front of the harbour, which has required dredging operations regularly. The large amount of sand required to be dredged has led to the harbour only being open 67 % of the time; in general, it is closed from December to March. The rough wave climate during these months has made it difficult to dredge since the dredging cannot be performed if the waves are higher than 1.5 meters. (Sigurdarson, 2016)

The accumulation of sediment inside the harbour basin was estimated before construction to be approximately 20,000 m³/year (Hjelmager Jensen, et al., 2007). However, in 2011 and 2012 the volume dredged was around 100,000 m³/year, which indicates that the volume in 2007 was underestimated.

4.3 Previous Studies

Several studies were carried out in the area around Landeyjahöfn, first to construct a well-functioning harbour, but subsequently to improve the existing harbour regarding the siltation problems. DHI has performed many of the studies, focusing on the sedimentations rates along the coast of Landeyjahöfn and also on the morphological changes with regard to the bathymetry and shoreline.

4.3.1 Morphological Evolution

4.3.1.1 Morphometric Changes of Shoreline

A variation in the shoreline position has been observed when studying the recorded evolution of the shoreline between the years 1954 and 2011. Far west of the harbour the shoreline has been rather stable as indicated by the small changes observed. Slightly west of the harbour, shoreline erosion of about 100 m occurred between 1954 and 2011. East of the harbour, the shoreline has experienced accretion of around 300 m during the same period. It is hard to decide a clear trend in the evolution east of the harbour, since there are many parameters affecting the sediment transport in this area. Large temporal variations could be expected by the fact that east of the harbour the river mouth of Markarfljót is located that supply the area with sediment, which varies depending on the volumes of meltwater (Elfrink, et al., 2006).

4.3.1.2 Morphometric Changes West of Landeyjahöfn

Detailed surveys have been performed over the last decade that illustrate the changes in the bathymetry around Landeyjahöfn. From 2002 to 2006, the surveys show that there is a pronounced longshore bar present with the crest at roughly 5.5-m depth immediately west of the harbour. About 2-3 km further to the west, the crest level is approximately at 4.5 m. Changes in the wave conditions during 2010 resulted in an increase in the westward sediment transport a landward movement of the longshore bar that filled the trough, causing a disappearance of the bar (Grunnet & Kristensen, 2013). Subsequently, a recovery of the bar occurred during 2011 and 2012, starting from the west and moving towards the harbour. The water depth at the bar to the west in 2012 was approximately 3.5 meters and it was 1 meter higher in the area 2-3 km west of the Landeyjahöfn Harbour compared to the area closer the harbour (Grunnet & Kristensen, 2013).

4.3.1.3 Morphometric Changes East of Landeyjahöfn

The areas east of the harbour does not show any clear trend of variation in the bar crest location other than a landward migration (2002-2006). The trough on the other hand experienced a depth change of 3 m under 2009-2012 due landward migration and filling in of the trough and bar. The areas closer to the harbour from the east side tend to be sensitive to the seasonal variation of the sediment supply from the river, which contributes to larger variation in the beach profiles over time. Several profiles east of the harbour tend to not have a bar, which can be explained by the strong slopes created near the river

mouth by sediment transport from Markarfljót (Grunnet & Kristensen, 2013). The bar observed near the river mouth has been referred to as a spit, since in some cases during the analysis the growth of this bar was analogous to a spit. The spit was growing from the river delta westwards, but the spit was never observed to reach the location of the harbour (Hjelmager Jensen, et al., 2007).

4.3.1.4 General Morphometric changes

To identify a trend in how the bar has moved or to predict how it will move, both with regard to the cross-shore and longshore direction, are difficult since the area has a complex sediment transport and changes occur on many scales. When studying the movement of the bar based on the measured bathymetries, the bar seems to have moved both east and west in an irregular manner. DHI, however, postulated an equilibrium between the bar/spit and the west-/east-going transport, but without defining this equilibrium (Grunnet & Kristensen, 2013). There are some conclusions made that may explain the situation, but they tend only to describe a small part of the whole system. This report also includes the analysis of the data to identify trends in morphometric properties.

4.3.2 Wave Climate

Offshore wave information was provided by Siglingastofnun from the years 1958 to 2012 (hindcasted from weather observations). The nearshore conditions were determined by DHI using the wave model MIKE 21 NSW (Near-Shore Waves). The model is a parameterized wind wave model that includes shoaling, refraction, growth due to wind, and dissipation due to white capping, breaking, and bottom friction. Results from MIKE 21 NSW showed that the nearshore wave climate is dominated by waves from the southeast and southwest.

As seen in Figure 11, locations further to the west are more exposed to high significant waves, which propagate from the southwest. Locations closer to Landeyjahöfn Harbour are exposed to milder wave climates, which is an effect of the sheltering provided by the Westman Islands. The wave roses also show that the areas to the west have two peaks in the distribution of wave direction, unlike the areas east of the harbour that have a one peak in the distribution of wave direction. (Grunnet & Kristensen, 2013)

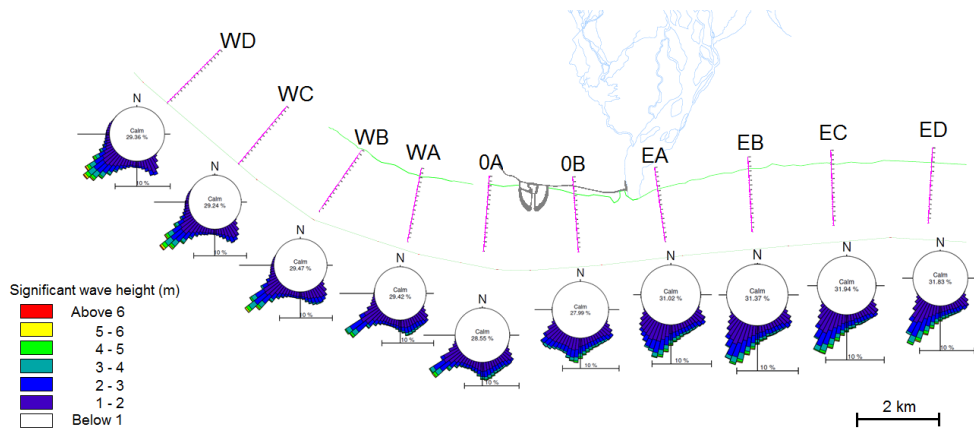


Figure 11: Wave climate for different locations from calculations by DHI. The roses show the waves direction distribution with consideration to the significant wave height. (Grunnet & Kristensen, 2013)

4.3.3 Sediment Transport

The combination of a sandy beach and the large waves propagating towards the coast give rise to large longshore sediment transport (LST) rates, where the wave angle plays a significant role for the transport magnitude and direction. The effect of the large LST and associated gradients can also be observed in the shoreline evolution, where the shoreline has been exposed to both erosion and accumulation. Shoreline changes depend on the variations in the wave climate, in time and space, inducing gradients alongshore that cause these changes. The sediment supply from Markarfljót is also a factor that affects the shoreline changes.

4.3.3.1 Overall sediment budget

DHI determined the sediment budget for the area around the harbour with regard to the littoral drift using the numerical modelling package LITPACK. LITPACK includes a deterministic LST model, which calculates LST rate as function of the local wave height, period, direction, loss of energy in the breaking, current speed and direction, and sediment properties. The sediment transport varies with the sediment grain size and the sediment density (Elfrink, et al., 2006). The input data used was from the nearshore wave calculations described in 4.3.2 encompassing a wave time series of 54 years.

Calculations were made to determine the littoral drift at the bar and the shoreline. Table 1 presents the resulting sediment budget for the different locations studied. The gross transport (Q_G) describes the absolute sum of the

west- and east-going sediment transport (Q_W , Q_E). The net transport (Q_N) is the sum of the west- and east-going transport taking into account the sign of the transport. Negative transport rate means that the sediment is transported to the east and positive to the west.

Profile	Position (km)	S_N (deg N)	Q_N (m ³ /yr)	Q_E (m ³ /yr)	Q_W (m ³ /yr)	Q_G (m ³ /yr)	$Q_{G,bar}$ (%)	$Q_{G,shore}$ (%)
WD	8.6	225	-230,000	-510,000	280,000	790,000	59	41
WC	6.6	220	-400,000	-640,000	240,000	880,000	60	40
WB	4.6	215	-180,000	-540,000	360,000	900,000	52	48
WA	2.6	191	-550,000	-1,040,000	490,000	1,530,000	43	57
0A	1.0	184	-620,000	-1,200,000	580,000	1,780,000	43	57
0B	1.0	176	-250,000	-670,000	420,000	1,090,000	23	77
EA	2.9	172	-590,000	-980,000	390,000	1,370,000	0	100
EB	4.8	177	-580,000	-1,030,000	450,000	1,480,000	0	100
EC	6.5	178	-780,000	-1,160,000	380,000	1,540,000	0	100
ED	8.5	183	-540,000	-990,000	450,000	1,440,000	0	100

Table 1: Summary of sediment budget derived by DHI. Position indicates distance from specific location to Landeyjahöfn Harbour. S_N is the shore normal of the profile at a specific location. Q_N is the net average annual LST rate. Q_E and Q_W are the calculated average annual LST rate towards east and west, respectively. Q_G is the gross LST rate. $Q_{G,bar}$ and $Q_{G,shore}$ give the contribution to the gross LST rate on the bar and at the shore, respectively. (Grunnet & Kristensen, 2013)

The results show that the net LST is dominated by sediment transported to the east. West of the harbour the littoral drift occurs both at the bar and at the shoreline, unlike the areas east of the harbour where the drift occurs adjacent to the shoreline. The explanation giving was that there is no bar present east of the harbour to produce a cross-shore LST distribution with two transport areas. Also, the calculated gross LST rates are larger east of the harbour compared to the west. At the harbour (mean value for locations 0A and 0B), the net LST rate is around 400,000 m³/year and the gross transport around 1,300,000 m³/year. (Grunnet & Kristensen, 2013)

The model calculations indicate that the variations in the westward and eastward LST are similar to the variation in the wave climate over the year. Thus, the net LST during the months May to September is small compared to the net LST during the months December to March. The seasonal variation shows that 68 % the annual gross LST occurs during the winter months. (Grunnet & Kristensen, 2013)

4.3.4 Evaluation of Radical Solutions

In Grunnet and Kristensen (2013) report, an investigation of five different radical solutions, where the aim was to improve the conditions at the harbour entrance with regard to siltation, were performed (Grunnet & Kristensen, 2013). These solutions are briefly reviewed in the following.

4.3.4.1 Radical Solution 1

The first solution is to construct an additional set of external breakwaters connected to the two existing breakwaters. The extension with the additional breakwaters has two possible layouts, one that has longer breakwaters than the other, see Figure 12. (Grunnet & Kristensen, 2013)

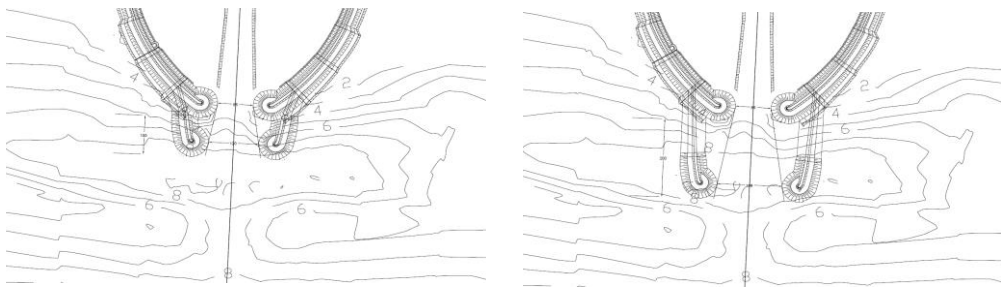


Figure 12: Radical solution 1 proposed by DHI. The solution includes two layouts, one with shorter and one with longer extended breakwaters. (Grunnet & Kristensen, 2013)

4.3.4.2 Radical Solution 2

The second radical solution is to create a constant seabed of 6-m water depth outside the harbour entrance. This solution is achieved by constructing a submerged berm with the dimensions 90 m wide and 240 m long, see Figure 13. (Grunnet & Kristensen, 2013)

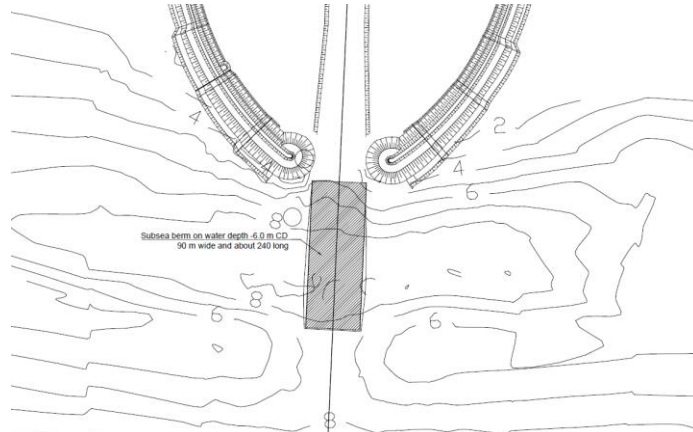


Figure 13: Radical solution 2 proposed by DHI. (Grunnet & Kristensen, 2013)

4.3.4.3 Radical Solution 3

The third radical solution includes the construction of two 600-m long detached breakwaters located outside the harbour. The opening between the breakwaters is 380 m and it is located in front of the entrance, see Figure 14. This solution has two different layouts; one where the breakwaters have crest levels at 2-m water depth and another where the crest level is 3 m above mean sea level. (Grunnet & Kristensen, 2013)

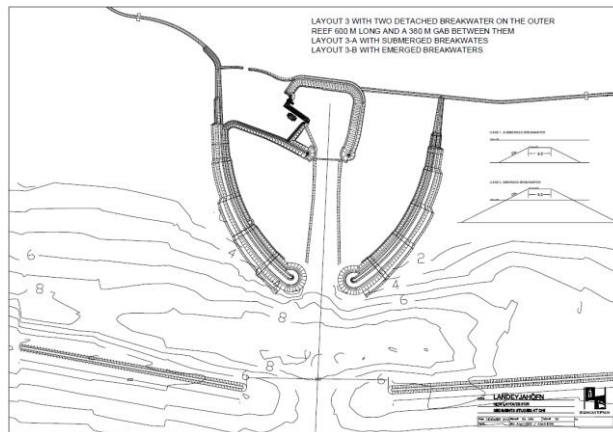


Figure 14: Radical solution 3 proposed by DHI. (Grunnet & Kristensen, 2013)

4.3.4.4 Radical Solution 4

The fourth solution is to construct sediment reservoirs (collection basins) on both the east and west side of the existing breakwaters. This solution is achieved through dredging operations, where the sizes of the reservoirs

depend on the LST rates. The eastward LST is larger than the westward and therefore a larger reservoir is needed on the west side, see Figure 15. The aim of this solution is to trap the sediment in the reservoirs before it reaches the harbour and therefore to reduce the bypassing capacity. (Grunnet & Kristensen, 2013)

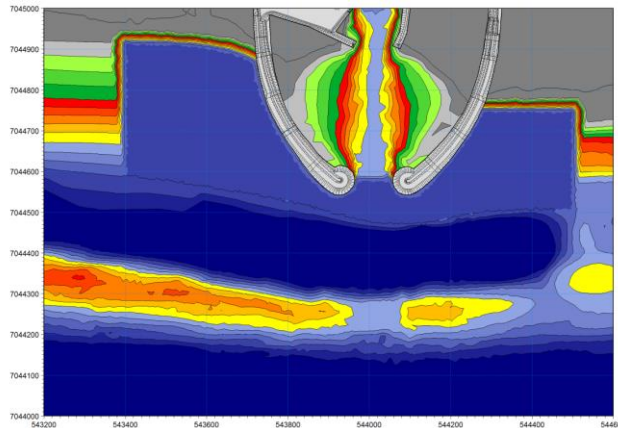


Figure 15: Radical solution 4 proposed by DHI. (Grunnet & Kristensen, 2013)

4.3.4.5 Radical Solution 5

The fifth radical solution is to retreat the shoreline by dredging a volume of 60,000 – 1,000,000 m³. The shoreline retreat would only be performed on the western side of the harbour, where the shoreline retreat would be 100 m, see Figure 16 (Grunnet & Kristensen, 2013). The aim of this solution is to increase the bypassing effect at the harbour entrance by further increasing the flow velocity due to additional contraction. (Grunnet & Kristensen, 2013)

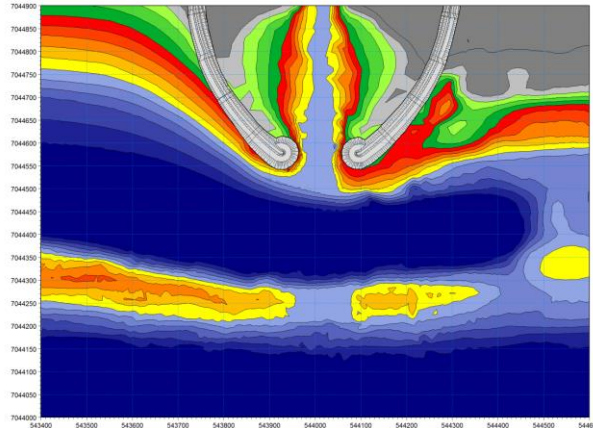


Figure 16: Radical solution 5 proposed by DHI. (Grunnet & Kristensen, 2013)

4.3.4.6 Conclusion of the Radical Solutions

DHI's analysis of the radical solutions showed that number 1, 2, and 5 did not imply significant improvement regarding the bypassing effect, which was the main aim of the solutions; therefore, these solutions are not preferable. Solutions 3 and 4, however, were shown to be potentially beneficial solutions with improvements of the bypassing conditions. However, further investigations should be made to evaluate if these solutions are sustainable. (Grunnet & Kristensen, 2013)

5 Data Compilation and Analysis

5.1 Bathymetric Data

The bathymetric data used for simulating wave transformation was taken from survey measurements done in February 2011. The data covers a large area outside Landeyjahöfn and gives an understanding of the how the bathymetry varies over the area, see Figure 17. To the east of the harbour the bathymetry is deeper than for the area to the west, 120 m and 70 m, respectively. At the Westman Islands shallow areas occur because of the influence of the islands.

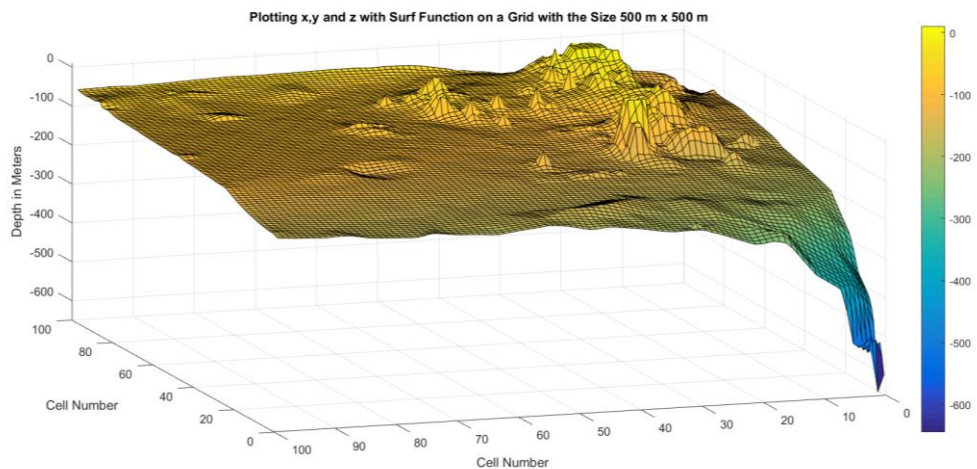


Figure 17: The bathymetry used in the simulation of wave transformation with the EBED model (from Matlab).

5.2 Wave Data

The input wave data employed consists of a long time series beginning in 1958 and ending in 2015 with values every 6th hour. This data includes the significant wave height, period, and direction hindcasted from weather data at an offshore location with coordinates 63°N 21°W, see Figure 18.

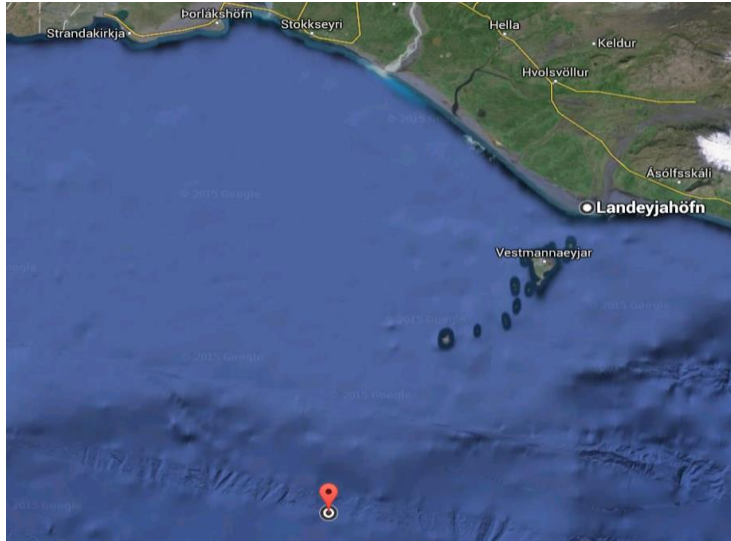


Figure 18: The offshore location from which hindcasted wave data was available with coordinates 63°N 21°W is shown by the red marker. (GoogleEarth, 2016)

In the figure below, Figure 19, a wave rose is shown with data from the hindcasted offshore location. The largest waves propagate from southwest with significant wave heights up to 14 m. In the figure the probabilities for specific propagation directions and significant wave heights are shown .

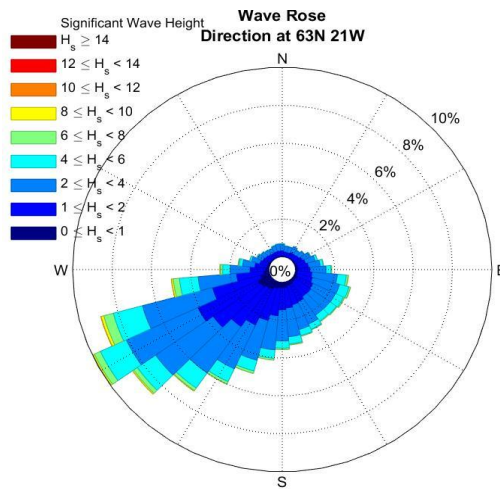


Figure 19: Wave rose for the significant wave height and direction hindcasted at an offshore location with coordinates 63°N 21°W.

5.3 Morphological Evolution

5.3.1 Morphometric Changes of Shoreline

To be able to see the long-term evolution of the shoreline a comparison was made based on four different years. Shorelines were available from the years 1908, 1966, 1989, and 2010 and were plotted in the same figure, see Figure 20. The reference system in which the data is measured is ISNET93.

Figure 20 shows that the areas to the west have been rather stable over the studied period, however the shoreline closer to the harbour from the west indicates marked changes over time, where the shoreline has migrated seawards. At the location of the harbour and to the east, an even larger change in the shoreline position can be observed, also indicating a seaward migration of the shoreline.

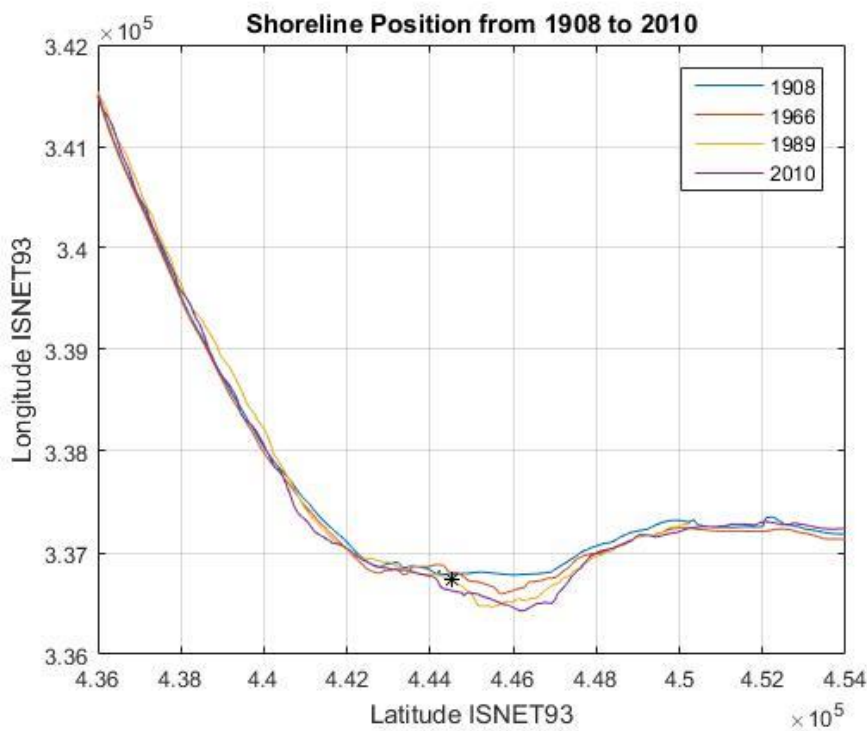


Figure 20: Shoreline position in the years 1908, 1966, 1989, and 2010 in the area around the harbour. The star presents the location of the harbour.

In Figure 21 the shoreline difference between 1966 and 1908, 1989 and 1966 and 2010 and 1989 is depicted. In Appendix 15.1 the shoreline differences are shown separately.

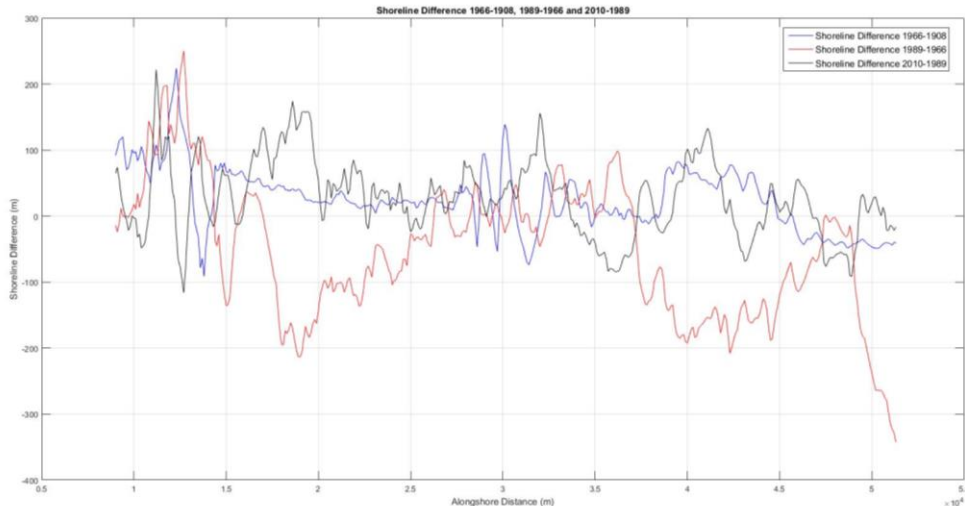


Figure 21: Shoreline differences between 1966 and 1908, 1989 and 1966 and 2010 and 1989.

5.3.2 Bar Evolution

The evolution of the bar is complex since the wave conditions and sediment transport around the harbour area vary at short time scales. As seen in Figure 22 the beach profiles measured in the section at the harbour exhibit large variations. These profiles show that in 2010 the bar disappeared due to changes in wave climate and the eruption, followed by a recovery in 2011 and 2012.

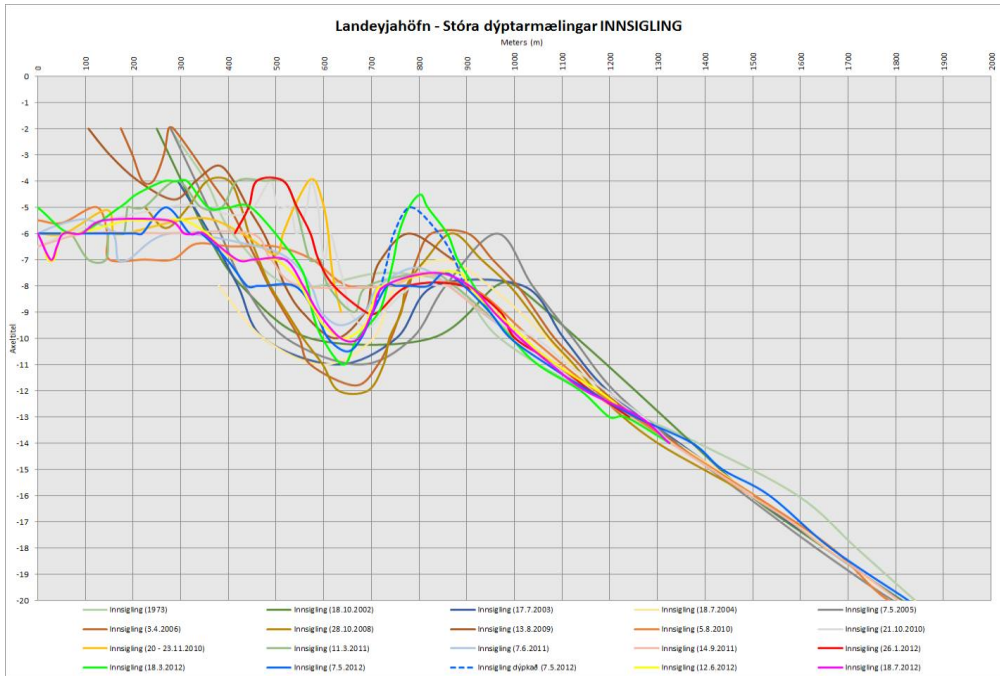


Figure 22: Beach profiles measured at a section located at the entrance of the harbour from 1973-2012.

6 Nearshore Wave Transformation

The model used to calculate the nearshore wave transformation is a numerical model called EBED (Mase, 2001). The model includes a detailed description of processes such as shoaling, refraction, breaking, and diffraction, and it is based on the conservation of wave energy flux. The input to the EBED model is the offshore wave conditions discussed previously.

6.1 Governing Equations

There are a set of equations used in the EBED model to describe the different wave transformation processes. The energy balance equation with diffraction and energy dissipation is written,

$$\frac{\partial(v_x S)}{\partial x} + \frac{\partial(v_y S)}{\partial y} + \frac{\partial(v_\theta S)}{\partial \theta} = \frac{\kappa}{2\omega} \left\{ (C C_g \cos^2 \theta S_y)_y - \frac{1}{2} C C_g \cos^2 \theta S_{yy} \right\} - \varepsilon_b S \quad (1)$$

where x and y are the coordinates, x points in the longshore direction and y in the cross-shore direction, v_x , v_y and v_θ are the propagation velocities in respective coordinate direction, S is the angular-frequency spectrum density, θ is the angle measured counter clockwise from the x -axis, κ is defined as an independent variable number applied to change the diffraction impact, ω is the angular frequency, C are the phase velocity, C_g are the group velocity and ε_b is a dissipation coefficient. (Sadabadi & Larson, 2012)

Following equation contains the different propagation velocities,

$$\{v_x, v_y, v_\theta\} = \left\{ C_g \cos \theta, C_g \sin \theta, \frac{C_g}{C} \left(\sin \theta \frac{\partial C}{\partial x} - \cos \theta \frac{\partial C}{\partial y} \right) \right\} \quad (2)$$

(Sadabadi, 2011)

The original EBED model often overestimated the wave height in the surf zone compared to measurements mainly due to the algorithm describing wave energy dissipation caused by wave breaking. Therefore, the energy dissipation term based on the Dally, et al. (1985) was introduced by Nam &

Larson (2010) in order to improve the predictive capability of the wave model in the surf zone. The modified energy equation is,

$$\frac{\partial(v_x S)}{\partial x} + \frac{\partial(v_y S)}{\partial y} + \frac{\partial(v_\theta S)}{\partial \theta} = \frac{\kappa}{2\omega} \left\{ (C C_g \cos^2 \theta S_y)_y - \frac{1}{2} C C_g \cos^2 \theta S_{yy} \right\} - \frac{K}{h} C_g (S - S_{stab}) \quad (3)$$

where K = dimensionless decay coefficient, h = still water depth and S_{stab} = stable wave spectrum density, which is a function of the stable wave height H_{stab} ($= \Gamma h$), Γ being a dimensionless empirical coefficient. (Nam & Larson, 2010)

Assuming that the spectrum density S and the stable spectrum density S_{stab} are functions of H_s^2 and H_{stab}^2 respectively, the dissipation term in Equation 3 (final term on the right-hand-side) can be rewritten as,

$$D_{diss} = \frac{K}{h} C_g S \left[1 - \left(\frac{\Gamma h}{H_s} \right)^2 \right] \quad (4)$$

(Nam, et al., 2009)

6.2 Model Input and Implementation

The input data needed to run the EBED model is the offshore wave conditions including the significant wave height H_s , significant wave period T_s and wave direction θ . The input could be measurements in a time series where each time step contains different wave conditions. The input data used here is the hindcasted waves from the offshore location 63°N 21°W. Other input data needed is the bathymetry and some general computational parameters (e.g., grid size, spectral resolution).

6.2.1 Bathymetric Data

The bathymetry is data from the measurements done in 2011, described previously. The measurements were done in the coordinate reference system UTM 27 V and the coordinates had to be rotated 310° to fit the set up of the model. The coordinates are converted so that the y-axis is parallel to the shoreline trend and the x-axis is perpendicular to this trend, see Figure 23.

Thereafter the grid is set up and its size is 100 x 100 cells, where each cell is 500 m x 500 m. All measurements were made on the seabed and no data for shallow areas or land areas was obtained. Thus, all parts of the bathymetry that had a depth less than 10 meters or was missing within the grid were set to negative values, which are treated as land in the EBED model. This was done to be able to simulate the influence of the Westman Islands on the wave transformation.

6.2.2 Wave Data

The input wave data is the hindcasted long time series of the significant wave height, significant wave period and wave direction. As mentioned before, the time series of input waves is 58 years long with values at six-hour intervals, that is, 12 am, 6 am, 12 pm, and 6 pm. The total number of waves in the series used as input in the model were 84,640. The data hindcasted at the offshore location was set as the boundary condition along the entire southern part of the grid in the EBED model.

To be able to use the input wave data for the EBED simulation, the wave angles were converted to the EBED system, where the in input angles to the model are defined as 220 degrees minus the wave direction true north, see Figure 23. Angles that are outside the range -90 to 90 degrees with regard to the grid are assumed not to affect the nearshore conditions and therefore neglected.

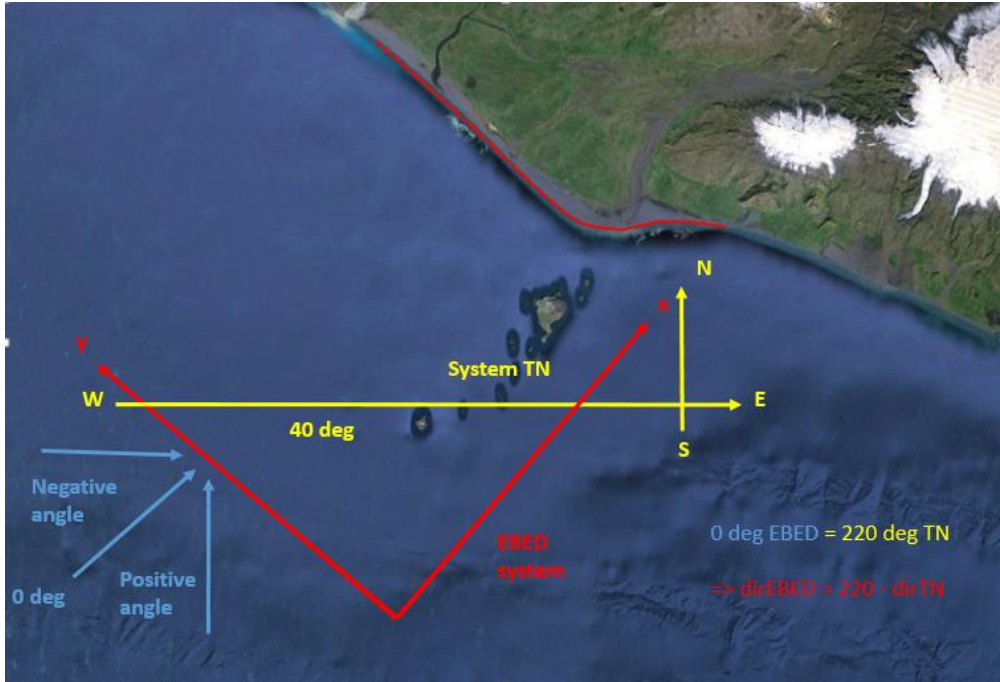


Figure 23: Definition sketch of the EBED grid. (GoogleEarth, 2016)

6.2.3 EBED Output Locations

Nine different output locations for waves were chosen along the boundary closest to the shoreline, see Figure 24. These locations were later used to simulate the LST rates as well as input to more detailed shoreline evolution simulations.



Figure 24: Output locations for the nearshore wave climate. (GoogleEarth, 2016)

6.3 Simulation Results

6.3.1 Wave Pattern EBED

The figures below illustrate the wave pattern for three different offshore wave inputs to EBED. The sheltering effect due to the Westman Islands can be observed in all the figures, where the influence varies with the incoming wave angle. Figure 25 presents the wave pattern when a wave enters the grid with a negative 45-degree angle. Figure 26 is the zoomed in area (the red box) in Figure 25 that presents the sheltering effect around the islands in more detail.

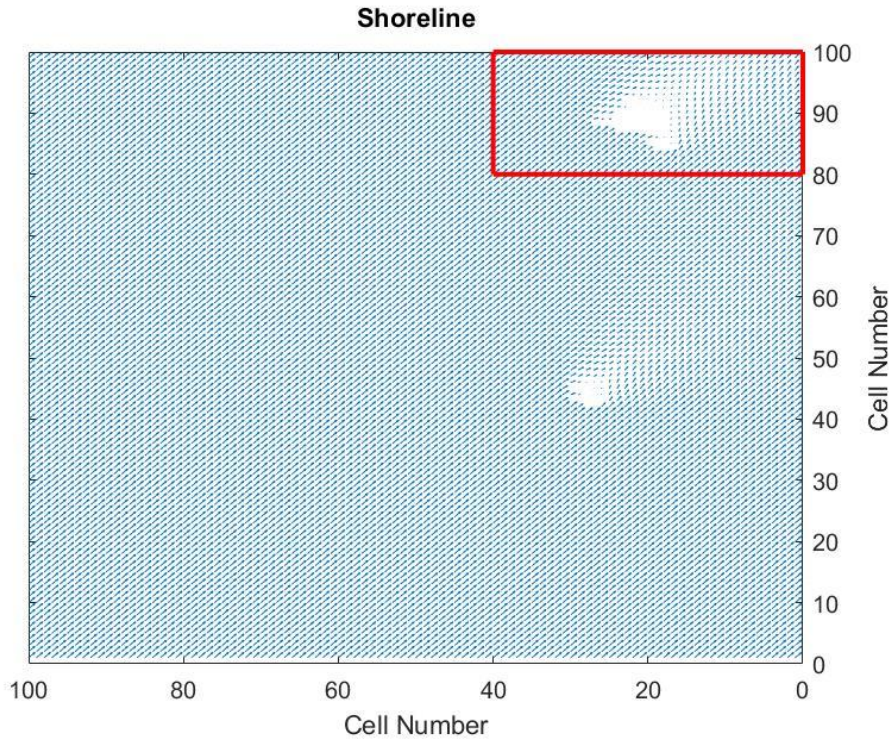


Figure 25: Illustration of the wave pattern for a wave with -45° deg incoming angle.

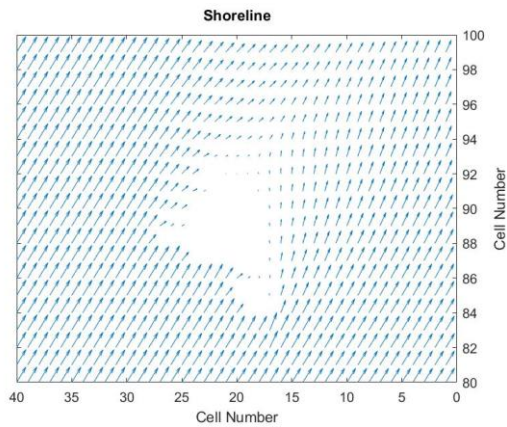


Figure 26: Illustration of the wave pattern for a wave with -45° deg incoming angle in the zoomed in red box.

Figure 27 presents the wave pattern when a wave is entering perpendicular to the EBED grid. Figure 28 is the zoomed in area (the red box) in Figure 27 that presents the sheltering effect around the islands in more detail.

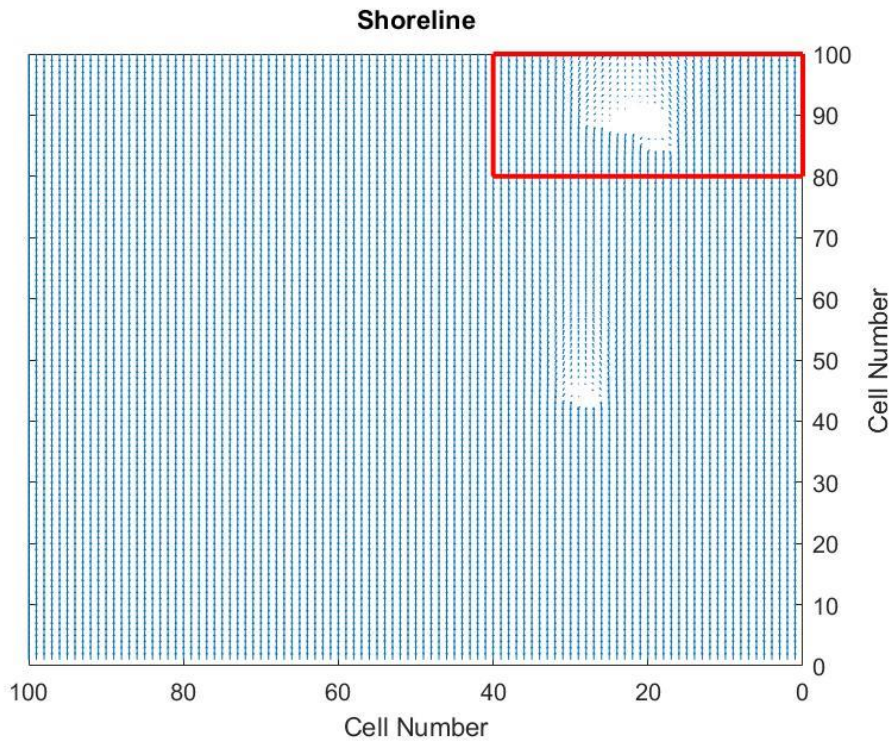


Figure 27: Illustration of the wave pattern for a wave with 0° deg incoming angle.

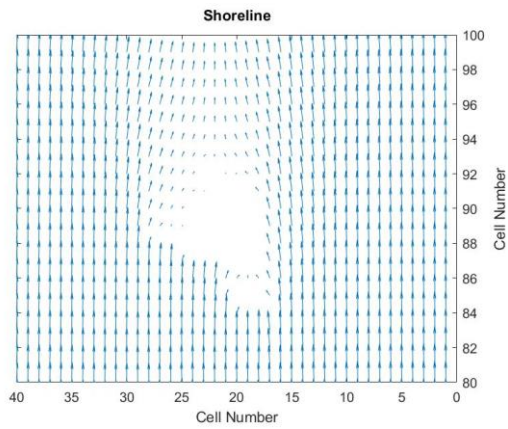


Figure 28: Illustration of the wave pattern for a wave with 0° deg incoming angle in the zoomed in red box.

Figure 29 presents the wave pattern with the incoming wave angle of 45 degrees. Figure 30 is the zoom in area (the red box) in Figure 29 that presents the shelter effect around the islands in more detail.

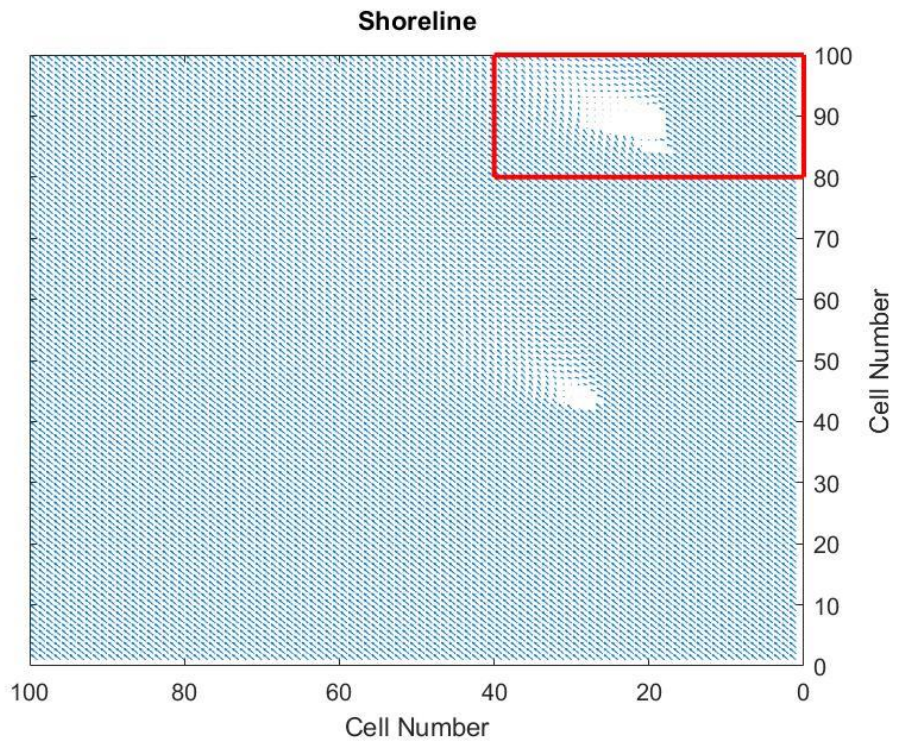


Figure 29: Illustration of the wave pattern for a wave with 45° deg incoming angle.

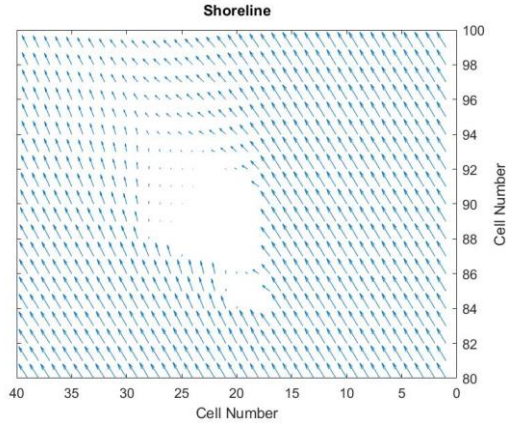


Figure 30: Illustration of the wave pattern for a wave with 45° deg incoming angle in the zoomed in red box.

6.3.2 Location Results

When running the EBED model the output was obtained for the nine selected locations along the shoreline. The output in each location was the nearshore wave climate including the significant wave height (H_s), significant wave period (T_s), and the wave propagation direction (θ). In Figure 31 the output is plotted as wave roses for each location.



Figure 31: Wave roses for the wave height and wave direction at each output location. (GoogleEarth, 2016)

In the following five figures, Figure 32, Figure 33, Figure 34, Figure 35, and Figure 36 the wave roses are magnified in order to more clearly show the wave climate at each location. As seen in these figures most of the waves propagate from southwest, but also some propagate from southeast. It is also possible to appreciate the sheltering effect from the Westman Islands, especially in Figure 33. In this figure, at location 3 the effect can be seen from southwest and at location 4 from south. Note that the figures may have different frequency axis.

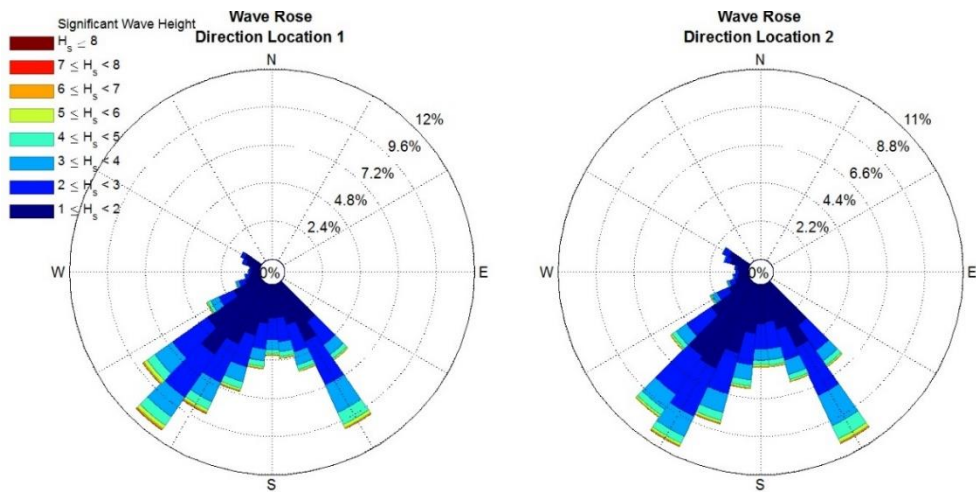


Figure 32: Wave height and wave direction at location 1 and location 2.

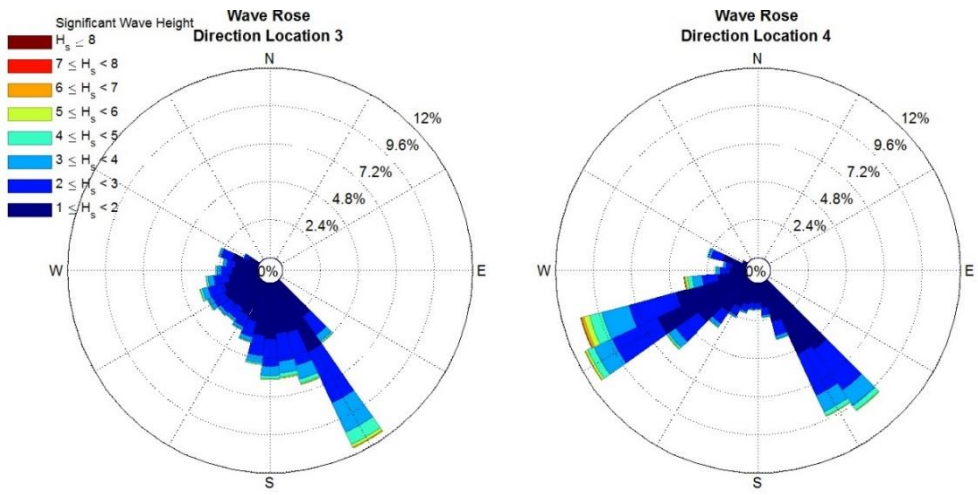


Figure 33: Wave height and wave direction at location 3 and location 4.

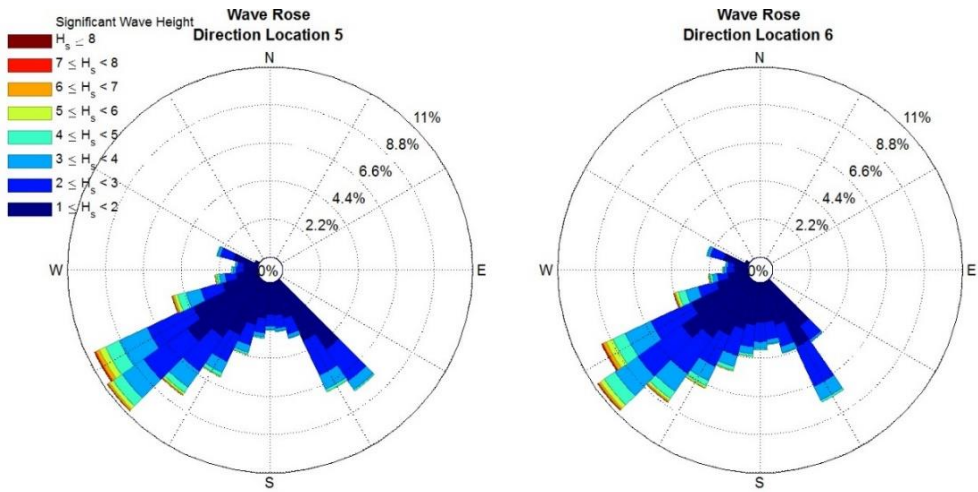


Figure 34: Wave height and wave direction at location 5 and location 6.

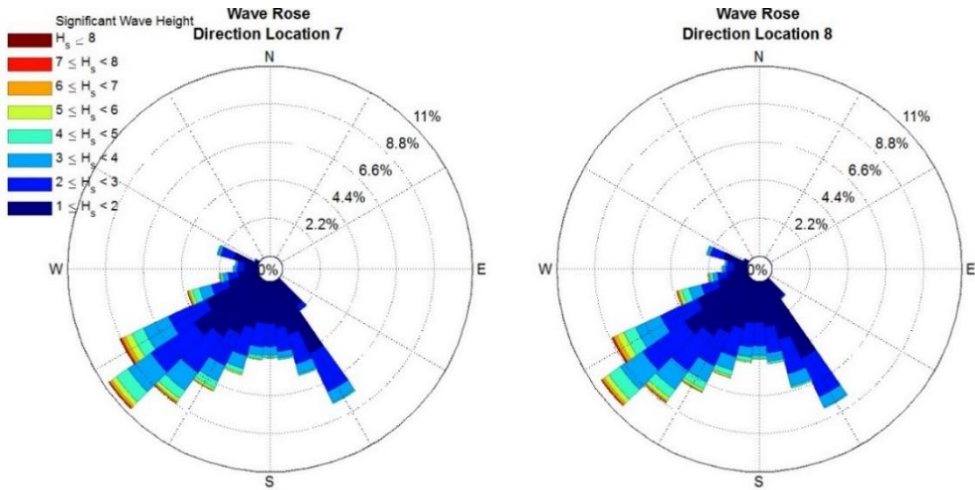


Figure 35: Wave height and wave direction at location 7 and location 8.

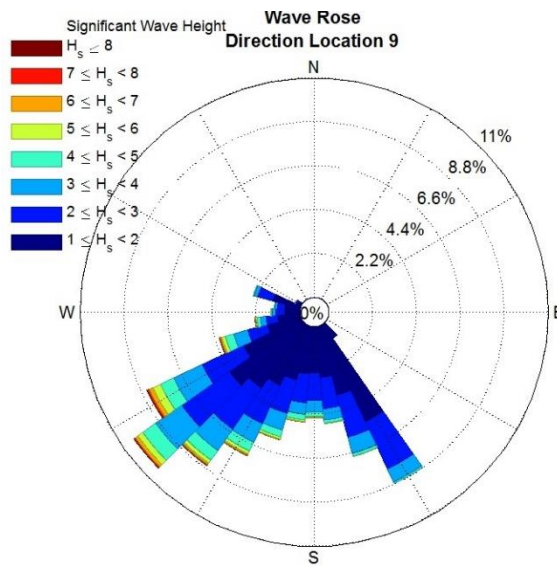


Figure 36: Wave height and wave direction at location 9.

6.4 Validation of Wave Model

When using a wave model for simulations the results should be tested with regard to its sensitivity towards different parameters. Also, model validation

should be performed by comparison with data, if possible, or towards other information on the general behaviour of the waves. Below are some discussions on these aspects of the wave modelling pertinent to the present study.

6.4.1 Extension of the Wave Model Grid

The location and extent of the wave model grid can be discussed, that is, if the grid should be expanded to the east to the better represent the sheltering effects from the Westman Islands when waves are coming from a sector east-southeast. To evaluate this limitation, the EBED model was run with a new, extended grid employing seven different wave conditions as input, see Table 2. The new grid extended 20 km to the east from the east boundary of the initial grid with a grid size of 100 x 140 cells compared to the initial grid size 100 x 100 cells, using the same cell size (500 m x 500 m).

Wave input	H_s	T_s	θ
1	3	7	-80
2	3	7	-45
3	3	7	-20
4	3	7	0
5	3	7	20
6	3	7	45
7	3	7	80

Table 2: Wave input conditions for test of the grid extension.

Four locations close to the harbour with the same position in both the initial model and the extended model were selected to evaluate the impact of the extension of the grid, see Figure 37. These locations were chosen because they are most probably affected by the sheltering effect from the Westman Islands.



Figure 37: Output locations in the wave model for evaluation of the grid extension. (GoogleEarth, 2016)

Wave Climate Results With and Without Extension of Grid

The results in Table 3, Table 4, Table 5, and Table 6 show that the extended wave model grid does not change the nearshore wave climate. The conclusion is therefore that the initial wave model grid can be used without any extension.

Location 1	Grid 100 x 100			Grid 100 x 140		
	H_s	T_s	θ	H_s	T_s	θ
1	2.09	6.89	-69.58	2.09	6.89	-69.58
2	1.9	6.8	-32.23	1.9	6.8	-32.23
3	2.2	6.97	-9.9	2.2	6.97	-9.9
4	2.42	7.06	5.72	2.42	7.06	5.72
5	2.54	7.07	21.66	2.54	7.07	21.66
6	2.59	7.03	41.15	2.59	7.03	41.15
7	2.6	7	61.66	2.6	7	61.66

Table 3: Wave model output at location 1 for initial grid (100 x 100) and extended grid (100 x 140).

Location 2	Grid 100 x 100			Grid 100 x 140		
Wave input	H_s	T_s	θ	H_s	T_s	θ
1	2.29	7.06	-72.13	2.29	7.06	-72.13
2	1.69	6.7	-38.32	1.69	6.7	-38.32
3	1.93	6.85	-6.28	1.93	6.85	-6.28
4	2.25	7.03	9.95	2.25	7.03	9.95
5	2.47	7.1	24.18	2.47	7.1	24.18
6	2.57	7.06	42.08	2.57	7.06	42.08
7	2.6	7	61.66	2.6	7	61.66

Table 4: Wave model output at location 2 for initial grid (100 x 100) and extended grid (100 x 140).

Location 3	Grid 100 x 100			Grid 100 x 140		
Wave input	H_s	T_s	θ	H_s	T_s	θ
1	2.71	7.04	-70.21	2.71	7.04	-70.21
2	1.93	6.96	-54.19	1.93	6.96	-54.19
3	1.56	6.61	-28.52	1.56	6.61	-28.52
4	1.57	6.59	9.9	1.57	6.59	9.9
5	1.89	6.92	34.14	1.89	6.92	34.14
6	2.28	7.12	48.91	2.28	7.12	48.91
7	2.5	7.05	63.34	2.5	7.06	63.35

Table 5: Wave model output at location 3 for initial grid (100 x 100) and extended grid (100 x 140).

Location 4	Grid 100 x 100			Grid 100 x 140		
Wave input	H_s	T_s	θ	H_s	T_s	θ
1	2.95	6.98	-66.78	2.95	6.98	-66.78
2	2.5	7.08	-43.94	2.5	7.08	-43.94
3	2.29	7.08	-28.51	2.29	7.08	-28.51
4	1.96	6.91	-14.56	1.96	6.91	-14.56
5	1.64	6.67	8.48	1.64	6.67	8.48
6	1.64	6.77	48.39	1.64	6.77	48.39
7	2.05	7.14	70.34	2.05	7.14	70.34

Table 6: Wave model output at location 4 for initial grid (100 x 100) and extended grid (100 x 140).

6.4.2 Input Boundaries and Wave Energy

The input on the offshore boundary can be discussed, whether it is enough to have only one input wave conditions along the entire boundary. However, the present EBED version does not allow for varying the input wave along the boundary. This is not a serious limitation for smaller grids; however, the larger the grid becomes, the more important it may be to allow for a spatially varying wave input at the offshore boundary.

Another issue concerning the EBED model and its offshore boundary conditions is the directional wave energy that the grid will allow to enter the model domain. Most nearshore wave transformation models are half-plane models, implying that only wave directions ± 90 degrees with respect to the offshore boundary can enter into the model domain. Since the grid is typically oriented with regard to the main trend of the coast, this is typically not a problem. The waves neglected, if they can propagate into the domain, would be small near the coastline and have large angles to the shoreline. From a sediment transport point of view, they might be neglected. However, this will to some extent depend on the local coastline orientation. The orientation of the EBED grid is such that waves from the southeast can enter, but moving counter-clockwise and approaching east the incoming wave energy from these directions will be restricted.

Some models may have lateral boundary conditions that does not allow free flow of energy into the model domain, but EBED employs a no-gradient in the energy spectrum meaning that energy enters (and leaves) the domain freely at the lateral boundaries. This can be observed in Figure 38, where the

wave pattern over the EBED grid with a wave input propagating from the southeast (135 degrees true north) is presented. The wave energy from southeast wave can move through the model grid. Figure 39 present the zoomed in area in Figure 38 (red box) showing the sheltering effect around the Westman Islands.

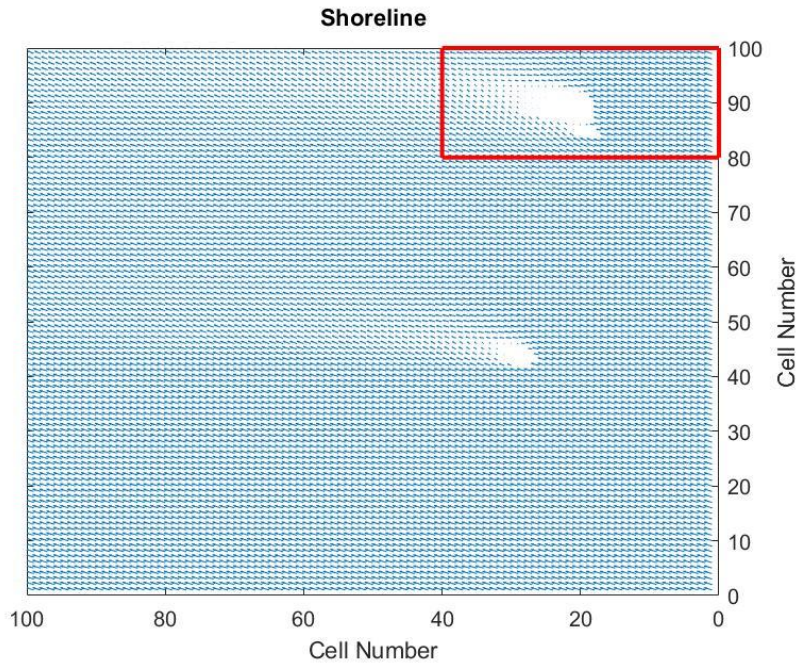


Figure 38: Wave pattern in EBED where the input wave is from southeast (135° true north). The blue arrows present the direction of the propagation of the wave. The top corner is the boundary of the grid towards the shoreline. The red box presents the zoomed in area present in the figure below.

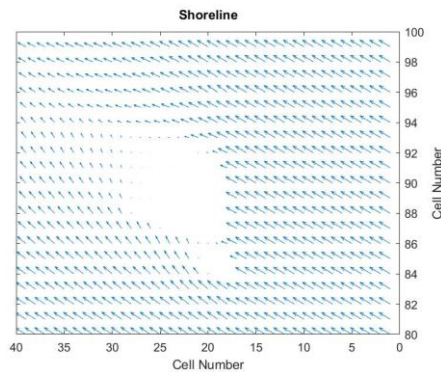


Figure 39: Illustration of the wave pattern for a wave with 135° true north incoming angle in the zoomed in red box.

6.4.3 Cell Size

The cell size of 500 m x 500 m employed influences the resolution of the bathymetry, especially around the Westman Islands, since the depths in the cells closest to the Westman Islands are hard to determine. The depths are interpolated between the closest measurements around and within each cell.

Because of the difficulties to simulate the influences of the Westman Islands another error may occur in the model. To be able to simulate the islands all depths less than 10 meters were set as -10 meters. As seen in Figure 38 there are only two major islands visible, due to the coarse bathymetric grid, but in fact the Westman Islands consist of 18 islands. Because of the resolution used and the absence of some of the Westman Islands, the simulations may include some errors, but the main islands are considered and their effects on the wave climate are reproduced.

7 Longshore Sediment Transport - Qtrans

To calculate the LST rate a model called Qtrans was used. The formula employed to calculate the LST rate is the CERC equation as described by the U.S. Army Corps of Engineers, 1984.

7.1 Governing Equations

The governing equation in the model is based on the assumption that the volume of sand transported alongshore per unit time, Q_{lst} is proportional to the longshore wave power per unit length of the beach and given by,

$$Q_{lst} = \frac{\rho K \sqrt{g/\gamma_b}}{16(\rho_s - \rho)(1 - a)} H_{s,b}^{2.5} \sin(2\theta_b) \quad (5)$$

where Q_{lst} is the LST rate in volume per unit time, ρ is the density of water, K is an empirical transport coefficient, g is acceleration due to gravity, γ_b is the breaker index ($= H_b/h_b$) that is set to 0.78, ρ_s is the density of sand, a is the porosity index ($\cong 0.4$), $H_{s,b}$ is the significant wave height at breaking and θ_b is the wave breaking angle. (Bayram, et al., 2007)

The output from the Qtrans model, when applied to a time series of waves, is the LST rate in the positive direction, the LST rate in negative direction, the net LST rate (sum of the positive and negative transport rates), and the gross LST rate (absolute sum of the positive and negative transport rates). Positive LST is taken towards the west and negative LST towards the east. A summation is done to obtain the average LST rates over different periods, typically on an annual basis. Gradients in the LST rate indicate movement of the shoreline, that is, if sediment is transported away or to a particular area. More output is given by Qtrans, including the wave height and angle at breaking for every wave in the time series.

7.2 Model Input and Implementation

The shoreline is divided into 12 sections due to the difference in the shoreline orientation, see Figure 40. The orientation of the shoreline sections was estimated from Google Earth images. The different sections have specific wave climates that are determined by where they are located with respect to the grid and the 9 wave output locations, which are presented in Table 7. The

model uses the nearshore wave time series, that is, the EBED results, for each location. When running the model, the shoreline orientation and the water depth where the waves are obtained are input to the calculations.



Figure 40: Definition sketch of the shoreline sections. (GoogleEarth, 2016)

Section	Wave Climate No.	Grid Point	Shore Angle (degrees)	Normal (degrees)	Length (m)	Depth (m)
1	1	1	97	187	2500	123.86
2	2	10	95	185	2500	98.89
3	2	10	90	180	2500	97.06
4	3	20	77	167	2500	44.83
5	3	20	95	185	2500	46.91
6	4	30	101	191	2000	80
7	4	30	123	213	3000	79.71
8	5	40	133	223	5000	60.88
9	6	50	135	225	6250	47.44
10	7	65	134	224	7500	48.64
11	8	80	131	221	8750	52.91
12	9	100	129	219	5000	57.80

Table 7: Shoreline section data.

7.3 Calibration of Transport Coefficient

The transport coefficient (K) that is used in the Qtrans model can vary from location to location depending on the properties of the area. Therefore, an evaluation of the transport coefficient in the CERC formula is needed for the study area.

7.3.1 Methodology

Measured shorelines were used to estimate the change in the shoreline position during a specific period. If the shoreline change (retreat < 0 and advance > 0) is Δy , assuming a beach profile that moves in parallel to itself with an active height D , the volume change per length shoreline is $\Delta y D$. Thus, for a shoreline stretch Δx , the total volume change will be $\Delta y D \Delta x$. The shoreline change is a result of the difference between the transport in and out (ΔQ) to the stretch over the studied period (Δt); thus, $\Delta Q = \Delta y D \Delta x / \Delta t$, where the transport represents an average over the studied period.

After ΔQ has been determined for a certain stretch a comparison was performed with the corresponding calculated ΔQ_{calc} , that was based on a coefficient value of $K = 0.2$ (Wang & Kraus, 1999) in the CERC formula.

The calibration of K is achieved with the relationship $K_{opt} = K\Delta Q/\Delta Q_{calc}$. This means that calculated Q -values based on K may be adjusted by multiplying them with a factor K_{opt}/K to achieve the best agreement with observations.

In the following this methodology is employed to derive K_{opt} for the study area on the south coast of Iceland. The analysis was performed in a somewhat schematic manner, estimated certain quantities visually; to achieve better estimate the analysis might be carried out at a greater detail.

7.3.2 Results

The shorelines measured 1908 and 2010 were used in the analysis. Figure 41 below depicts these two shorelines together with the calculated difference between the shorelines, where $\Delta y > 0$ denotes shoreline advance (accumulation).

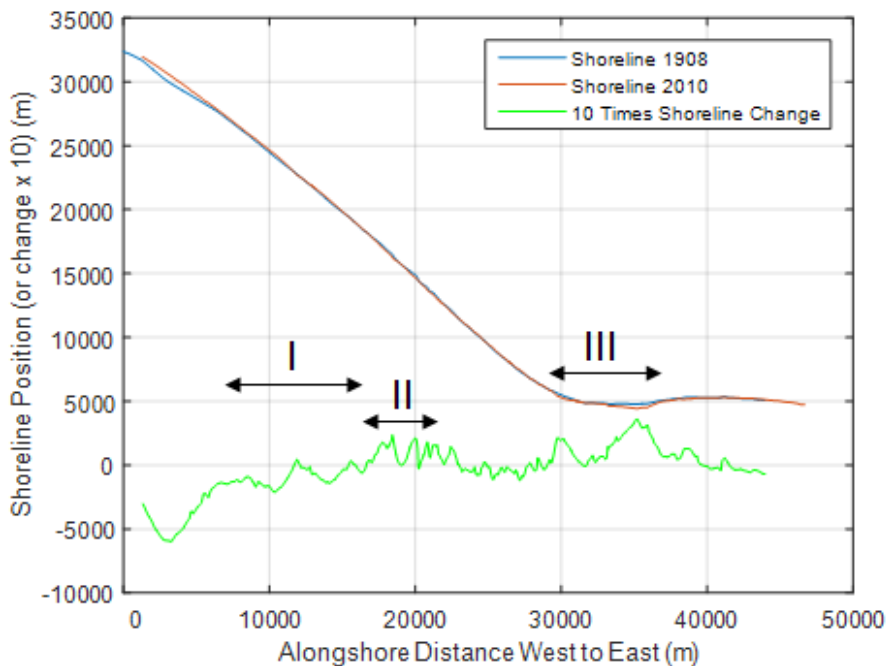


Figure 41: Shoreline change between 1908 and 2010. Green line presents the shoreline difference multiplied with factor 10. Positive values indicate accumulation and negative erosion.

Three sections with reasonably uniform response were identified for further analysis (Figure 41). The accumulation zone immediately to the east was not included, since it is anticipated that sediment discharge from the river has affected shoreline evolution in this area. After ΔQ was estimated, the relevant ΔQ_{calc} from the previous calculations was used to determine K_{opt} . The result of the analysis is briefly summarized below.

Section 1: Erosion was observed in this area with an average retreat of about 99 m along a stretch of 10,000 m ($6,230 < x < 16,230$). With an active profile height of 15 m (depth of closure 12 m + berm height 3 m; compare study in Portugal (Baptista, et al., 2014)) the eroded volume is $\Delta V = 99 \cdot 10,000 \cdot 15 = 14.9$ million m^3 . To calculate the yearly net transport out from this section ΔV is divided by Δt yielding $\Delta Q = 140,000$ m^3 /year. From the previous Q -calculations, the transport in and out from this is approximately 0.3 and 0.2 million m^3 /year, respectively, which gives a net out of $\Delta Q_{calc} = 100,000$ m^3 /year (transport direction defined as before). Thus, $K_{opt} = 0.2 \cdot 140 / 100 = 0.28$.

Section 2: Accumulation was observed in this area with an average advance of about 89 m along a stretch of 5,000 m ($16,230 < x < 21,230$). With the same active profile height, the accumulated volume is $\Delta V = 89 \cdot 5,000 \cdot 15 = 6.7$ million m^3 , yielding $\Delta Q = 65,000$ m^3 /year. From the previous Q -calculations, the transport in and out from this section is approximately 0.2 million m^3 /year and 0 million m^3 /year, respectively, which gives a net in of $\Delta Q_{calc} = 200,000$ m^3 /year. Thus, $K_{opt} = 0.2 \cdot 65 / 200 = 0.065$.

Section 3: Accumulation was observed in this area with an average advance of about 160 m along a stretch of 7,410 m ($29,320 < x < 36,730$). With the same active profile height, the accumulated volume is $\Delta V = 160 \cdot 7,410 \cdot 15 = 17.8$ million m^3 , yielding $\Delta Q = 174,000$ m^3 /year. From the previous Q -calculations, the transport in and out from this section is approximately 0.55 million m^3 /year and 1.3 million m^3 /year, respectively, which gives a net out of $\Delta Q_{calc} = 750,000$ m^3 /year. Thus, $K_{opt} = 0.2 \cdot 174 / 750 = 0.046$.

7.3.3 Concluding Remarks

Three quite different values on K_{opt} was obtained for sections I, II, and III, namely 0.28, 0.065, and 0.046, respectively. The average of these three

values gives $K_{opt} = 0.13$. However, the value estimated for section I is probably more uncertain since the input sediment transport to the section is difficult to estimate. Using only the values from sections II and III yield $K_{opt} = 0.056$, which might be a more realistic value. This value may be compared with studies in Portugal that obtained $K_{opt} = 0.039$ (Baptista, et al., 2014). To use the calibrated transport coefficient value 0.056, all previously calculated Q -values with the initial transport coefficient ($K = 0.2$) should then be adjusted by multiplying them with a factor $K_{opt}/K = 0.056/0.2 = 0.28$.

Shoreline data from 1966 and 1989 was also available, so analyses between the years 1908-2010 and 1966-2010 were performed to evaluate the transport coefficient. The results between 1908 and 1989 showed to be similar with result between 1908 and 2010 with an average $K = 0.04$ for sections II and III. The results between 1966 and 2010, however, differed compared to the other analyses, with an average $K = 0.095$. This value is rather large and would give gross sediment transport rate in the size range 2-2.5 million $m^3/year$, which is not reasonable and therefore this value was not taken into account. Even though the results from 1908 and 1989 are similar to the 1908 and 2010, the latter period will be used for the calibration of the transport coefficient. This selection is motivated by the fact that a long period is desirable when analysing shoreline changes.

7.4 Results

7.4.1 Sediment

Table 8 below presents the results of the LST calculations for the different sections. The gross transport (Q_g) describes both the west- and east-going sediment transport (absolute values). The net transport (Q_N) is the resulting transport of the west-going (Q_W) and east-going (Q_E) transport. Negative LST rate means that the sediment is transported to the east and positive to the west.

Profile	Q_E (m ³ /yr)	Q_W (m ³ /yr)	Q_N (m ³ /yr)	Q_G (m ³ /yr)
1	-750,000	550,000	-200,000	1,300,000
2	-600,000	500,000	-100,000	1,100,000
3	-650,000	450,000	-200,000	1,100,000
4	-350,000	250,000	-100,000	600,000
5	-300,000	500,000	200,000	800,000
6	-700,000	400,000	-300,000	1,100,000
7	-650,000	250,000	-400,000	900,000
8	-550,000	350,000	-200,000	900,000
9	-500,000	500,000	0	1,000,000
10	-500,000	500,000	0	1,000,000
11	-600,000	500,000	-100,000	1,100,000
12	-650,000	550,000	-100,000	1,200,000

Table 8: Summary of LST calculations for the 12 sections. Q_E and Q_W presents the LST rates towards east respective west. Negative values present LST rates towards the east and vice versa. Q_N presents the net LST rate and Q_G the gross LST rate. The rates are rounded off.

The results show that the general net LST is towards the east with rates varying from 0 to 0.4 million m³/year. The gross LST rates are in the range 0.6 to 1.3 million m³/year.

7.4.2 Net Sediment Transport

Figure 42 presents the regional pattern of the net LST. The sections far west and east of the harbour have low net transport rates, unlike the sections closer to the harbour on the west side that have larger net LST rates. At Section 5, where the harbour is located, the net transport is towards the west, which stands out from the other sections.



Figure 42: The regional net LST pattern. (GoogleEarth, 2016)

7.4.3 Gross Sediment Transport

Figure 43 below presents the gross LST for the different sections. The sections west and east of the harbour have a gross transport around 1 million $m^3/year$. The sections closer to the harbour have lower gross transport than the other sections.



Figure 43: The gross sediment transport pattern along the shoreline. (GoogleEarth, 2016)

7.5 Result Analysis

7.5.1 Net Sediment Transport

The regional net LST pattern is of interest to study since it indicates the large-scale evolution of the shoreline. Figure 44 presents the expected shoreline response with regard to the calculated net LST pattern. Between Sections 11 and 10 the results indicate that there will be accretion (Accretion I) since 0.1 million m³/year is transported in from Section 11 to 10 and that no sand is transported out of section 10, meaning that 0.1 million m³/year will deposit in the area. Sections 9, 8 and 7 indicate that erosion most probably will occur along the sections (Erosion I) since sediment is transported away from the sections. Between Sections 6 and 5 the net sediment transports both from east and west converge, which indicates that accretion and shoreline advance will occur here (Accretion II). The westward sediment transport in the harbour section is caused by the sheltering effect of the Westman Islands, since the waves propagating from the southwest are significantly reduced. Thus, the dominant transport is towards the west. The evolution at the sections east of the harbour are more complex because of the supply of sediment from the river Markarfljót and it is therefore hard to determine how the shoreline will change. However, since eastward transport is observed from Section 4 and downdrift, erosion will probably occur (Erosion II).

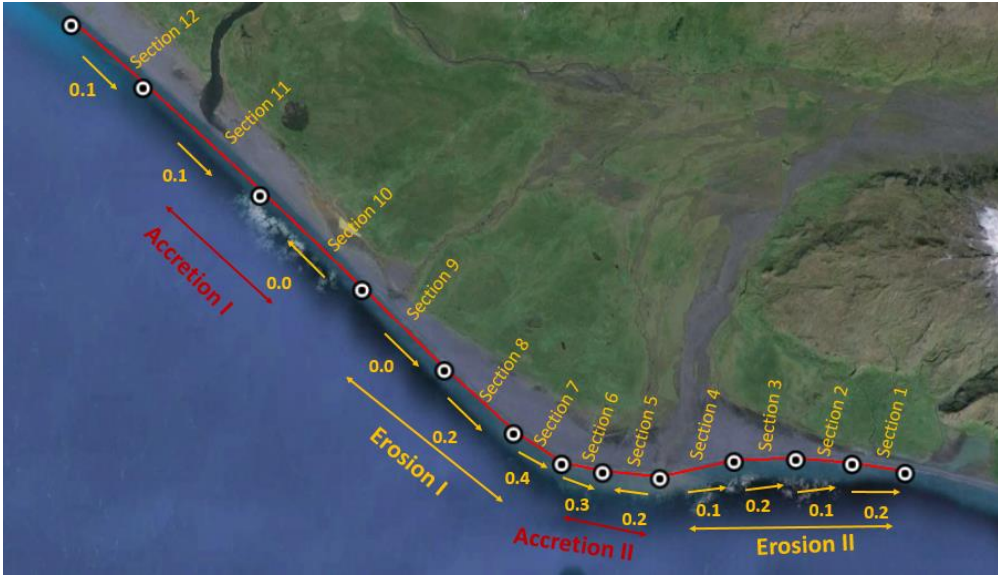


Figure 44: The expected large-scale evolution of the shoreline as a result of the calculated net LST pattern. (GoogleEarth, 2016)

The net LST rates from the Qtrans model are similar to the results from the LITPACK model, which Grunnet and Kristensen (2013) used in their study, regarding the general transport trend towards the east. However, the net transport rates were lower in the Qtrans model results, varying from 0 to 0.4 million $m^3/year$ (see Table 8), compared to the LITPACK model, which predicted rates of 0.2 to 0.8 million $m^3/year$ (see Table 1) in 4.3.3.1.

7.5.2 Gross Sediment Transport

When comparing the gross LST rates from the Qtrans model with the LITPACK model, a difference can be observed. LITPACK presents lower gross transport rates west of the harbour than east of the harbour. Qtrans on the other hand yields a lower rate at the section east of the harbour compared to west of the harbour. The LITPACK model has the largest gross transport rate slightly west of the harbour (profile OA; see Figure 11 in 4.3.2), 1.78 million $m^3/year$. This is of interest when evaluating the position of the harbour with regard to the probability of accumulation inside the harbour, since the gross transport has a large influence on this process (Hanson, 2015). The Qtrans model at the harbour (section 5) produces a gross transport rate of 0.8 million $m^3/year$, which is roughly 0.6 million $m^3/year$ less than corresponding

cross-sections OA and OB in the LITPACK-model. Overall, the lower gross LST rate in this area depends on the sheltering effect of the Westman Islands.

7.5.3 Comparison Between Qtrans and DHI's Litpack

In Grunnet and Kristensen (2013) report the LST rates from the profiles OA, WB, and OB by the LITPACK model were presented in diagrams to show the yearly net transport trend. The rates from these profiles are compared below with the output from Qtrans that match the location of the profiles. It is not straightforward to perform this comparison, but it was made to get an overview of the differences between the model results.

Figure 45 below presents the net LST rate from year to year for the area approximately 5 km west of the harbour. The top figure is from Grunnet and Kristensen (2013) report covering a period from 1958 to 2012 for the WB profile and the bottom figure is the result from the Qtrans model from 1958 to 2015 for Section 7. The patterns of the net LST rate from both of the models are rather similar.

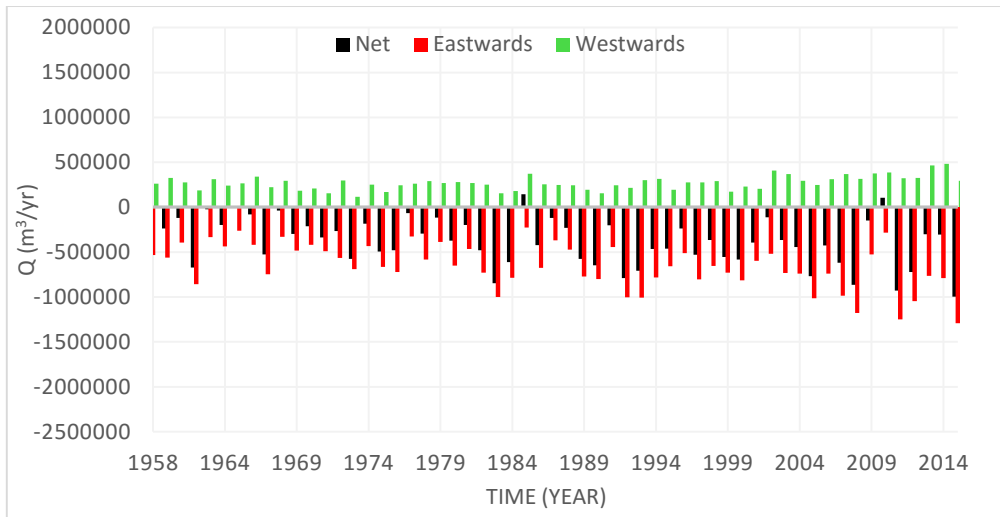
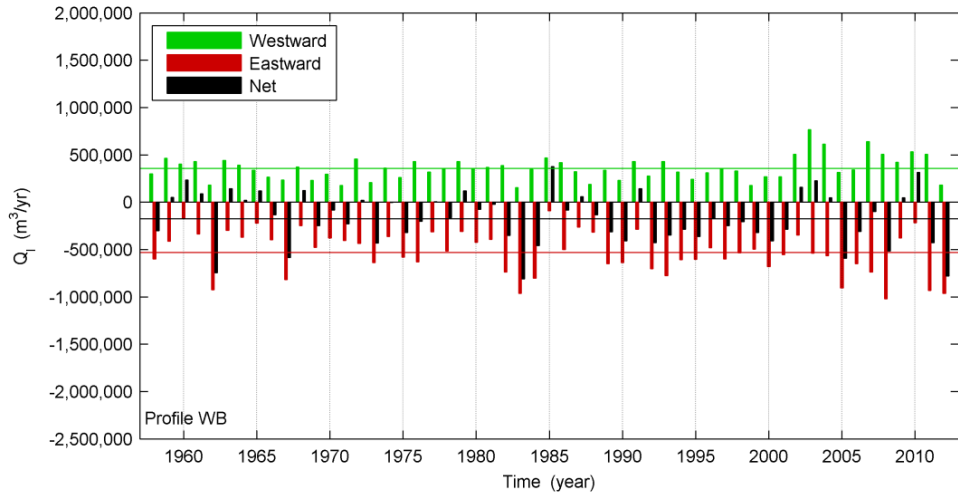


Figure 45: Net transport variation over time for profile WB from the LITPACK model (top) and section 7 from the Qtrans model (bottom). The green bars show the yearly sediment transport towards the west and the red bars towards the east; these two components are summarized in net transport (black bar).

Figure 46 below presents the net LST rate from year to year in the harbour area. The top figure is from Grunnet and Kristensen (2013) report covering the period from 1958 to 2012 for the OA profile and the bottom figure is the result from the Qtrans model from 1958 to 2015 for Section 5. The models show quite different results for this section; the LITPACK model predicts a dominant net LST to the east, whereas the results from Qtrans yield a dominant net LST westwards.

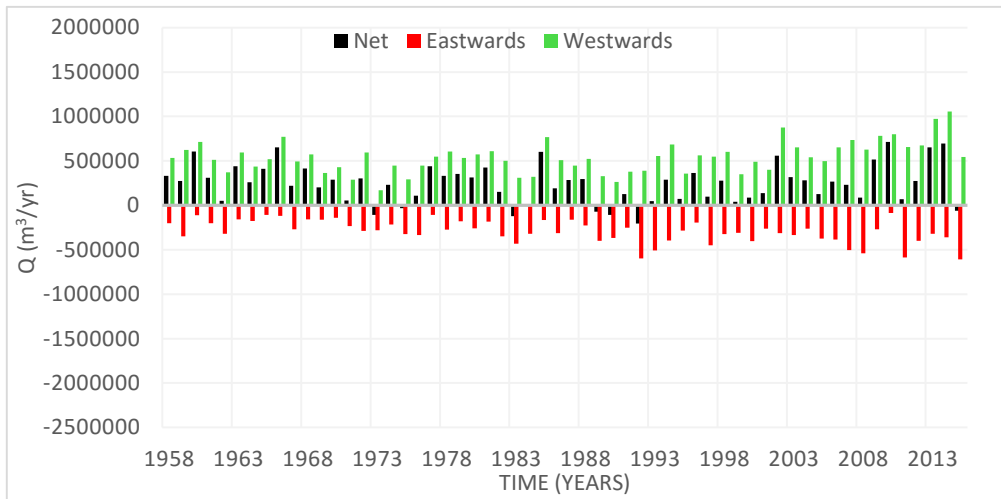
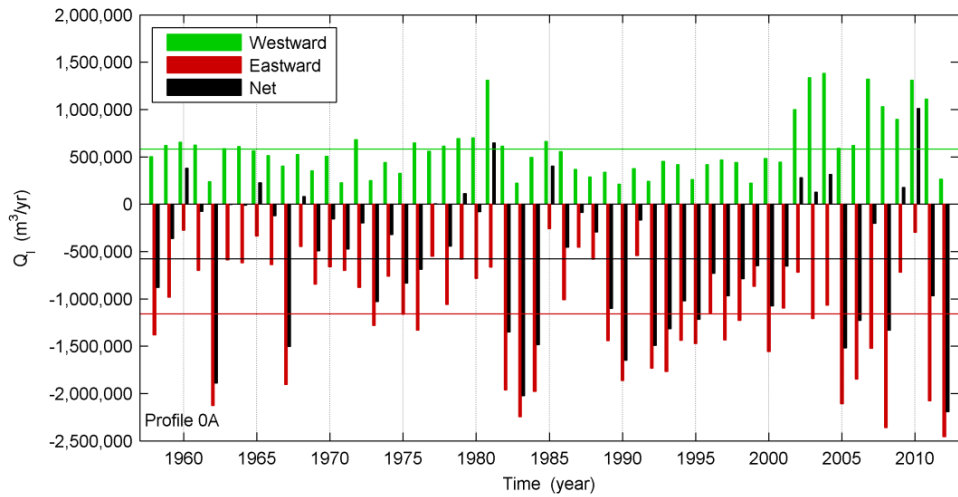


Figure 46: Net transport variation over time for profile OA from the LITPACK model (top) and section 5 from the Qtrans model (bottom). The green bars show the yearly sediment transport towards the west and the red bars towards the east; these two components are summarized in net transport (black bar).

Figure 47 below presents the net LST rate from year to year for the area roughly 5 km east of the harbour. The top figure is from Grunnet and Kristensen (2013) report covering the period 1958 to 2012 for the EB profile and the bottom figure is the result from the Qtrans model from 1958 to 2015 for section 4. The transport patterns of the net LST rate from both models are

rather similar. However, the LITPACK model presents a more dominant eastward transport compared to the Qtrans model.

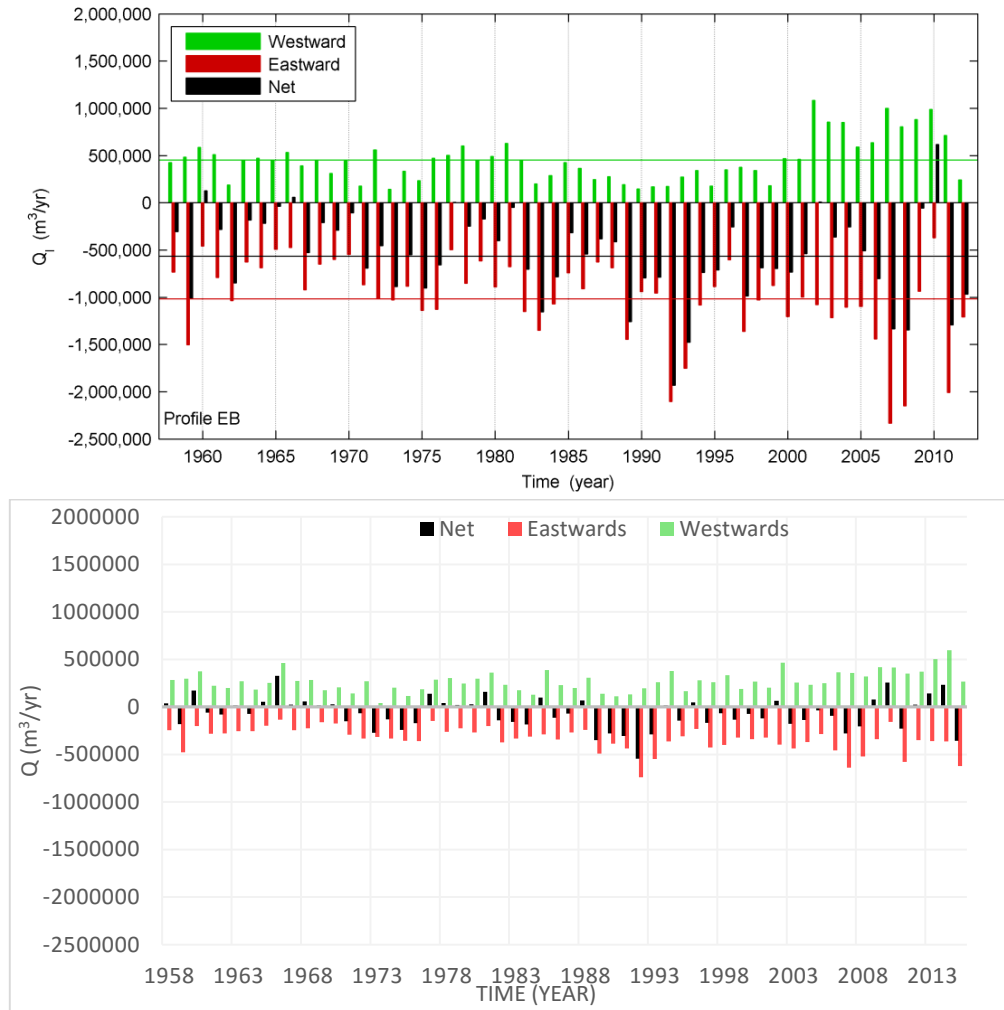


Figure 47: Net transport variation over time for profile EB from the LITPACK-model (top) and section 4 from the Qtrans-model (bottom). The green bars show the yearly sediment transport towards the west and the red bars towards the east; these two components are summarized in net transport (black bar).

8 Long-term Coastal Evolution – Cascade

8.1 Governing Equations

After the schematic calculations with Qtrans, which gave an idea of the large-scale LST pattern and associated shoreline evolution, additional modelling was performed to resolve more details of the LST and the resulting shoreline change. The model employed is called Cascade and it was developed to simulate regional sediment transport and coastal evolution. The model can be applied to stretches of coastline where primarily LST controls the evolution and where time scales extending to centuries may be of interest. Since major coastal projects typically are associated with large time and space scales, a regional model may be needed to display the full consequences and interaction of man-made structures and activities with natural processes. (Larson, et al., 2002)

The model includes several phenomena such as inlet creation, ebb- and flood-tidal shoal development, bypassing bars between beaches and inlets, channel dredging, regional trends in the shape of the coast, relative change in sea level, wind-blown sand, storm impact, longshore bar formation, periodic beach nourishment, and shore-protection structures such as groins and seawalls. Here an open coast is modelled with no inlets, implying that not all these features are included.

The longshore sediment transport is given by Equation 6, (Palalane & Larson, 2016).

$$Q_{lst} = \frac{\varepsilon}{(\rho_s - \rho)(1 - a)gw} F\bar{V} \quad (6)$$

where F is wave energy flux directed towards shore, \bar{V} the longshore current velocity (surf zone average), ε an empirical transport coefficient, ρ_s (ρ) the sediment (water) density, a the porosity, and w the sediment fall speed. An empirical expression was developed for ε based on the dimensionless fall speed from a large data base. However, preferably ε should be established through calibration. A comparison between Equation 6 and the CERC formula, employing the mean longshore current in the surf zone due to breaking waves, yields for small angles at breaking $\varepsilon = 0.77c_fK$, where K is

transport rate coefficient in the CERC formula and c_f the bottom friction coefficient. In this derivation an equilibrium beach profile was employed using the relationship between the shape parameter and fall speed from Kriebel, Kraus, and Larson (1991). (Palalane & Larson, 2016)

Gradients in the LST cause corresponding movement in the shoreline position, which typically dominates the long-term response. However, sediment movement onshore and offshore also cause the shoreline to move seawards or landwards. For example, the shoreline movement is affected by the exchange between the bar and berm, dune erosion, and wind-blown sand. Material exchange between the bar and berm region occurs at different time scales because of changes in the seasonal wave conditions. This exchange between the bar and the berm is assumed to take place under conservation without any material being lost offshore. In Cascade, individual bars are not described, but the volume eroded from the berm is stored in only one offshore bar complex (Larson *et al.*, 2013). This bar will achieve a certain equilibrium volume (V_{BE}), if the forcing conditions are steady. However, if the bar volume (V_B) at any given time is smaller than V_{BE} , then the bar volume will grow, whereas $V_{BE} < V_B$ causes a decay in bar volume. A growth in V_B causes a corresponding decrease in berm volume (shoreline retreat), and vice versa (shoreline advance). (Palalane & Larson, 2016)

There are four different types of boundary conditions formulated in Cascade: no transport ($Q = 0$), no shoreline change ($\partial Q / \partial x = 0$), bypassing, and bypassing and inlet sediment storage and transfer (for the two later boundary conditions, Q is derived in submodels). (Larson, et al., 2002)

Bypassing at groins may occur in the model and the bypassing ratio is calculated based on the geometrical blockage of the cross-shore distribution of the LST. Thus, this distribution has to be estimated updrift the groin. The groins will have an effect on the shoreline movement, due to the blocking of sediment. (Palalane & Larson, 2016)

8.2 Model Input and Implementation

Cascade is employed to calculate the coastal evolution at the regional scale. The wave input applied is the output from the EBED model, i.e., the nearshore wave climate containing the significant wave height H_s , the significant wave period T_s , and the wave direction θ . The number of waves in

the input time series are 65,743, corresponding to the hindcasted waves at the offshore location used in the EBED simulations. The nine different output locations from the EBED model were used as wave input to Cascade, allowing for varying wave conditions along the grid; for each specific location an individual depth was set, see Table 9.

The number of cells employed in the Cascade grid was 209, where each cell was 200 m long. The grid started east of the harbour and extended to the west (thus, grid point 1 is furthest to the east). The median grain size was set to 0.4 mm. The studied shoreline stretch was divided into two larger sections to be able to use different transport coefficients along the grid. These coefficient values were based on the results discussed in 7.3.3 and a calibration of the shoreline evolution between 1966 and 2010. The depth of closure and the height of the berm were set to 12 m and 4 m, respectively. A source describing the sediment supply from the river east of the harbour was included and set to 100,000 m³/year (Sigurdarson, 2016). Bar evolution was included in the simulations, making it possible to obtain the bar volume in time at specific locations along the shoreline.

No.	Position on the grid	Depth (m)
Wave climate 1	1	145
Wave climate 2	10	95
Wave climate 3	22	50
Wave climate 4	25	87
Wave climate 5	35	61
Wave climate 6	55	47
Wave climate 7	100	49
Wave climate 8	155	52
Wave climate 9	209	59

Table 9: Position of input wave climates from EBED along the Cascade grid.

8.3 Calibration Cascade

A calibration of the model was performed to make the model fit the observed shoreline evolution from 1966 to 2010, a period for which wave and shoreline data was available. Several input parameter values were tested and changed during the calibration such as median grain size, depth of closure, and berm height. The most difficult part of the calibration was to select the value of the CERC transport coefficient. The value was at first set to 0.056

along the entire shoreline. As seen in Figure 48 the model calculated a larger retreat and advance than what the observed shoreline displayed (note that the shoreline is viewed from the sea in the figures; the x -axis of the model runs in the western direction and the y -axis point offshore). The model also had some difficulties to simulate the evolution in the area west of the harbour because of the large shoreline orientation. Even if a certain smoothing of the shoreline is possible to apply in the model when calculating the wave transformation, a large shoreline orientation may still be difficult to handle.

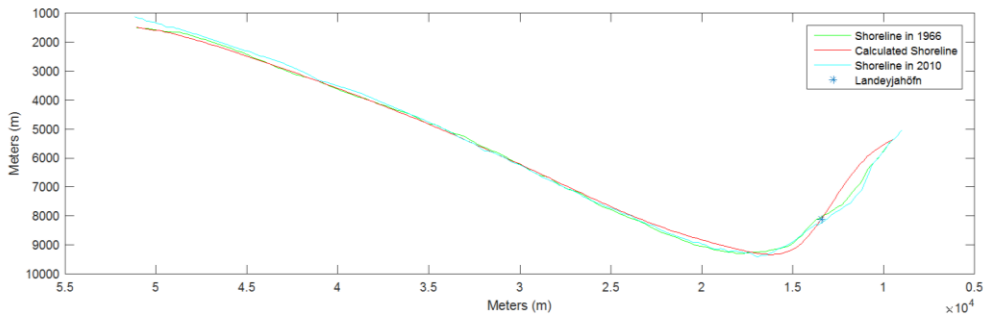


Figure 48: Calculated shoreline evolution with Cascade using a transport coefficient of $K = 0.056$ along the entire shoreline.

In order to improve the simulated shoreline evolution, keeping in mind the results of the previous analysis with Qtrans and the observed evolution, the transport coefficient was allowed to vary spatially. The calibration involved specifying the value on the transport coefficient at two nodes from which coefficient values were interpolated at individual nodes along the grid. The first specified value was 0.01 at node 30 and the second was 0.056 at node 210; between node 30 and 210 linear interpolation was employed, whereas between node 1 and 30 the constant value from node 30 was used. The low value at node 30 was needed to avoid the pronounced evolution around the harbour obtained with a higher transport coefficient.

8.4 Simulation Results

The Cascade model generates a wide range of outputs. The outputs are: the shoreline at specified times, the longshore transport rate at specified times, the inlet shoal volumes during the simulation (not relevant here), the average longshore transport rate, the cross-shore features during the simulation at specified locations.

The LST rates predicted by the model is depicted in Figure 49.

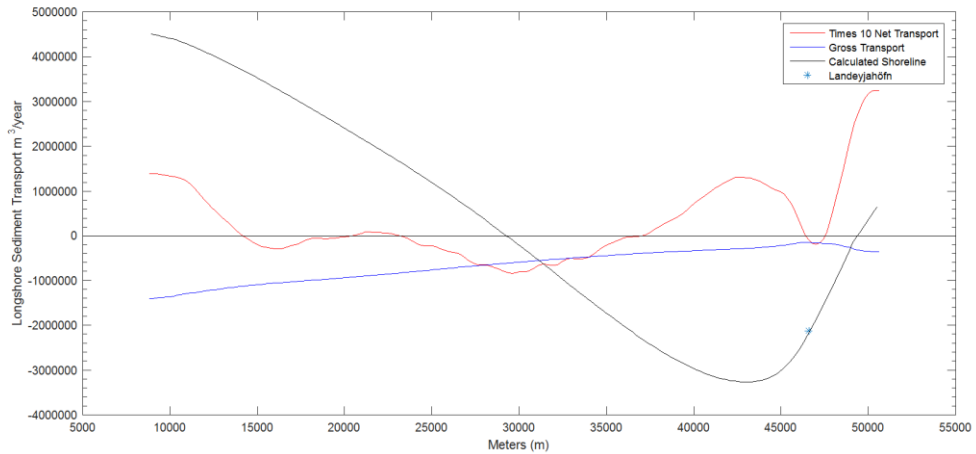


Figure 49: Calculated LST rates with Cascade for the case of a spatially varying transport coefficient (positive values are transport eastwards and negative values westwards).

Figure 50 shows the simulated shoreline evolution with the Cascade model from 1966 to 2010 using values on the transport coefficient that vary in space as described before. The measured shoreline 2010 is also shown together with the location of the harbour marked with an asterisk.

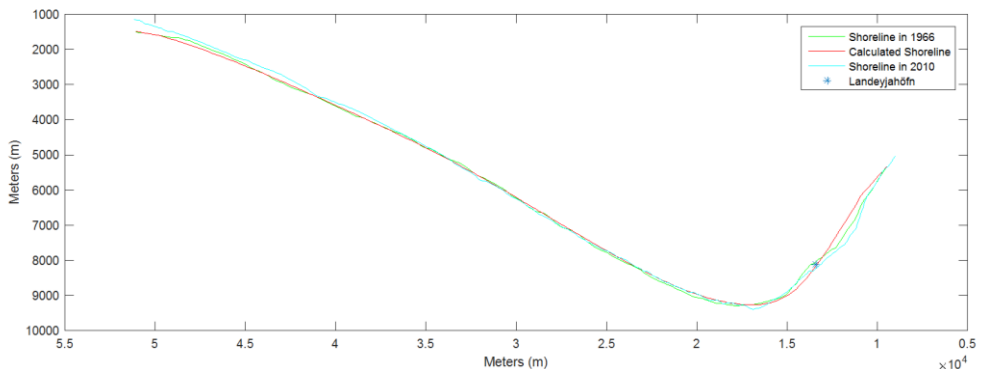


Figure 50: Results from simulation of the shoreline evolution 1966 – 2010 with the Cascade model using a spatially varying transport coefficient.

As seen in Figure 50 the model results are in good agreement with the measurements for the calibration simulations. Particularly the shoreline evolution west of the harbour is well described, reproducing the stable behaviour observed here, which also supports the simulated wave climate

with EBED. The section around the harbour it more difficult to assess, partly because of the influence of the river Markarfljót. Since the river mouth have shifted over the years it makes the area less stable and complicates the modelling. The sediment supply from the river was estimated to be around 100,000 m³/year, as discussed before.

8.5 Result Analysis and Comparison with Qtrans

The pattern of the net LST rates in both the models, observed in Figure 42 and Figure 49, show similar trends. However, due to the calibration of the Cascade model, which focused on achieving a good fit with the observed shoreline evolution, the comparison of the LST rates between the two models was not straightforward. Lower LST rates were simulated by the Cascade model due to lower transport coefficient values being used. However, similar trends can still be observed in the results from the two models. To the west of the harbour in both models low net LST appear, indicating that the shoreline is rather stable here. Closer to the harbour from the west a clear eastward LST is predicted by both models. At the harbour section, the LST is westwards in both models. East of the harbour it is hard to assess the result from the models, due to the complexity of the influence of the river. However, eastward transport is seen in all the sections.

9 Bar Evolution Analysis

9.1 Comparison of Bathymetries and Sediment Transport

A comparison between some of the more distinct bathymetric features and the sediment transport calculated by the model Qtrans was made. The bathymetries analysed in the comparison was those that had a clear difference between two subsequent dates, separated by a period no longer than five months. Thus, five different time intervals of interest were identified. The sections of significance in the study were Sections 4, 5, and 6, which are close to the location of the harbour. Section 4 is east of the harbour, Section 5 by the harbour, and section 6 west of the harbour, see Figure 51. The sediment supply from the river Markarfljót was not taken into account in the Qtrans model.



Figure 51: Sections 4, 5, and 6 in the vicinity of the harbour employed in the bathymetric analysis. (GoogleEarth, 2016)

Table 10 below presents the five different periods investigated and the net calculated LST for Sections 4, 5, and 6 (transport is representative for the entire specific section).

Start Date	End Date	Section 4 (m ³)	Section 5 (m ³)	Section 6 (m ³)
26 th Jan. 2012	7 th May 2012	-142,000	-96,000	-452,000
19 th Nov. 2012	16 th Mar. 2013	236,000	650,000	272,000
9 th May 2014	29 th Jul. 2014	-18	22,000	-2,000
13 th Oct. 2014	18 th Jan. 2015	-71,000	9,000	-360,000
18 th Jan. 2015	7 th May 2015	-285,000	-170,000	-712,000

Table 10: Results from the Qtrans model for the investigated periods and sections of interest. Positive values are transport towards west and negative values towards east.

As seen in Table 10 the sediment transport was eastwards in the period 26th of January 2012 to 7th of May 2012, which is validated by looking at the bathymetries in Figure 52, where the bar west of the harbour clearly experienced a growth towards the east. Also, by comparing the beach profiles, see Figure 22 in 5.3.2, from the same period they show that the bar volume by the harbour increased with 400 m³/m. The wave rose at the top right in Figure 52 shows that the largest and most of the wave propagated towards east during this period, which the sediment transport indicates.

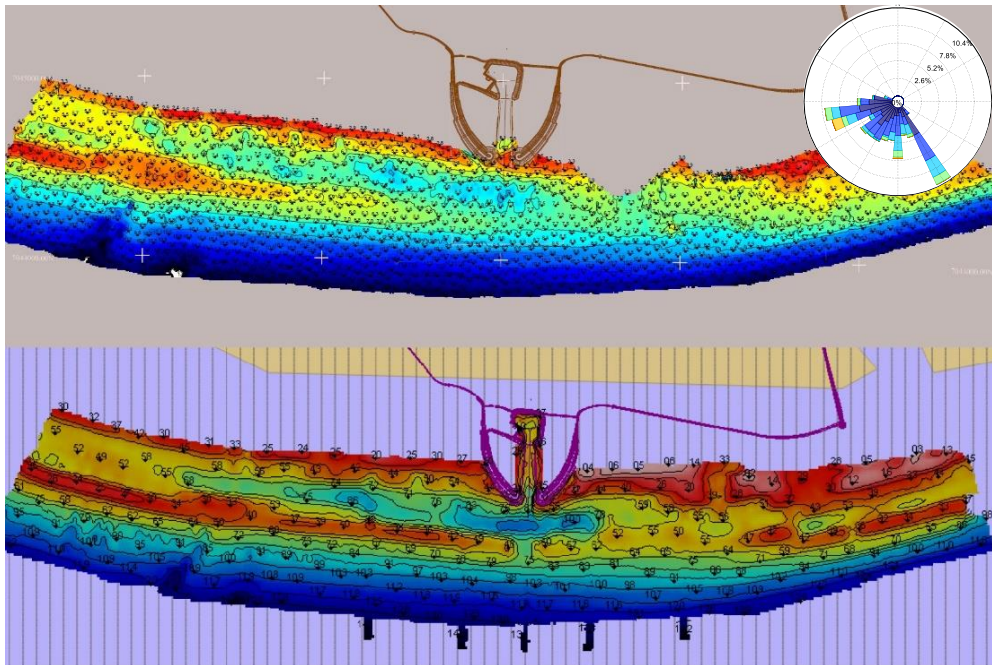


Figure 52: The measured bathymetries on the 26th of January 2012 and 7th of May 2012.

Figure 53 displays the changes in the bathymetry during the period from 19th of November 2012 to 16th of March 2013. As seen in the figure, the growth in this period, especially east of the harbour, was towards the west, which is validated by the transports in Table 10. Seen in the top right in Figure 53 almost all of the waves propagated from south-southeast, which the sediment transport calculations indicate.

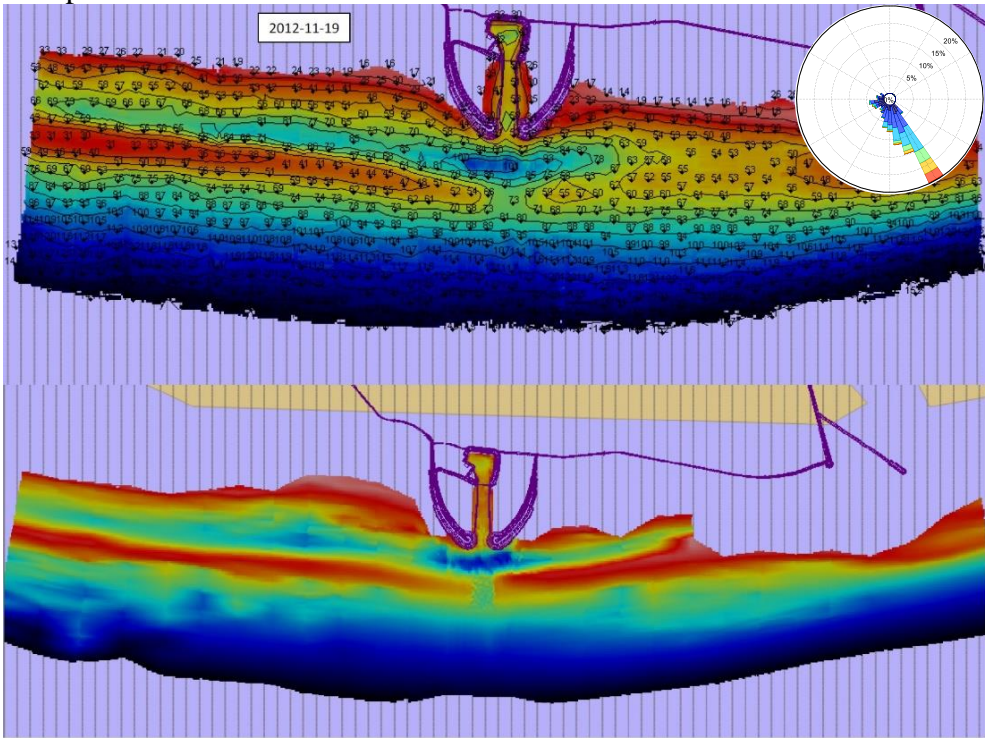


Figure 53: The measured bathymetries on the 19th of November 2012 and 16th of March 2013.

In Figure 54 it is harder to see a distinct difference between the bathymetries on the 9th of May 2014 and 16th of July 2014 as in the two previous cases; however, this is not surprising since the transport in Sections 4 and 6 quite small. In Section 5 the transport was westwards, although the transport rate was not as large as under the other periods analysed due to the calmer wave climate during the summer months. On the east side of the harbour sediment accumulated and the same effect is seen on the west side of the harbour. This response is confirmed by the calm wave climate during the period, also shown in Figure 54.

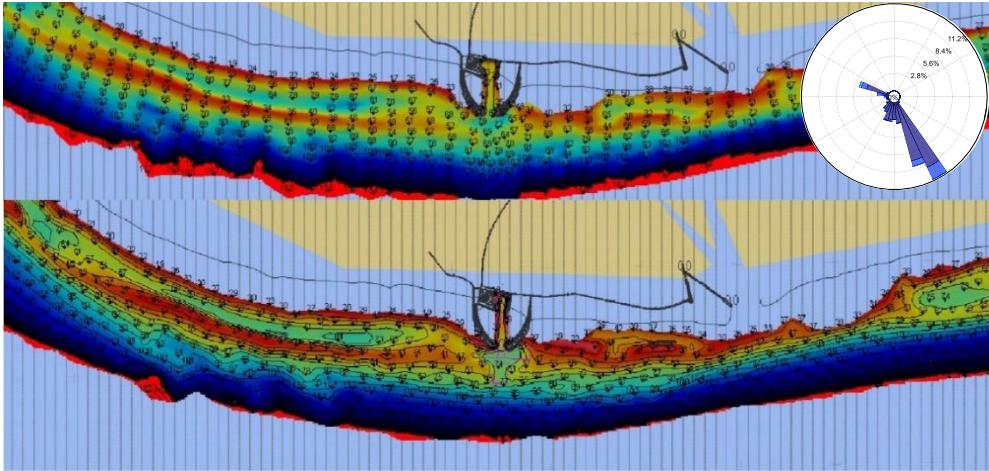


Figure 54: The measured bathymetries on the 9th of May 2014 and 29th of July 2014.

Table 10 indicates that there have been small movements of the bar to the east, in the period from 13th of October 2014 to 18th of January 2015, which can be observed in Figure 55 due to waves propagating from southeast. However, because of a fairly uniform wave climate from south, with largest waves from south-southeast, the formation of the bar might be explained, see the top right in Figure 55.

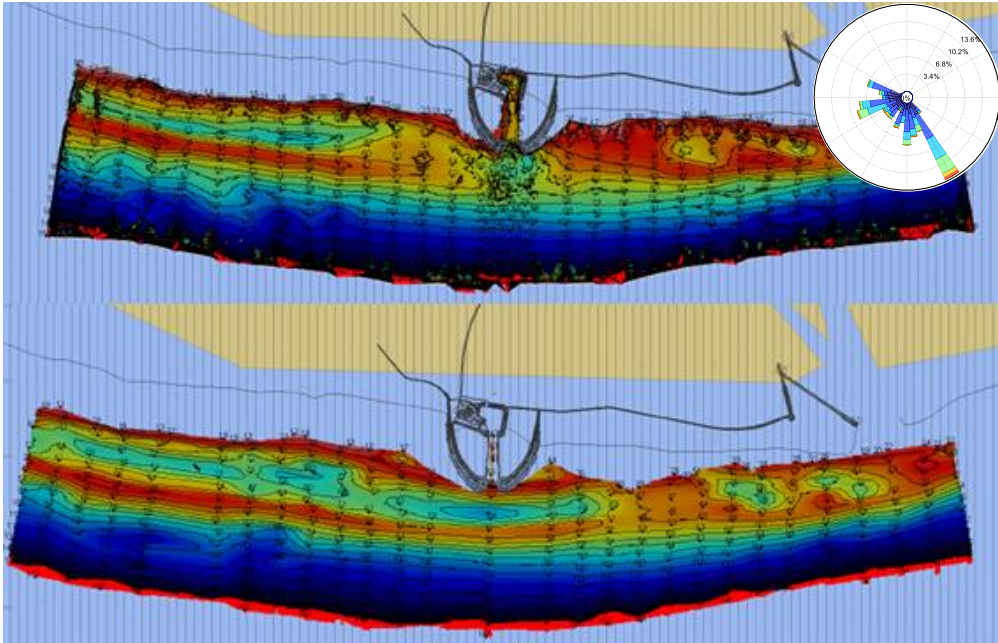


Figure 55: The measured bathymetries on the 13th of October 2014 and 18th of Jan. 2015.

For the period 18th of January 2015 to 7th of May 2015, Table 10 shows that the transport rates were eastward. The wave rose, at the top right in Figure 56, shows large waves propagating from south, which might be the reason for the distinct bar forming alongshore. Comparing the beach profiles at the harbour section from the same period, Figure 22 in 5.3.2, the bar is more distinct and has a larger volume.

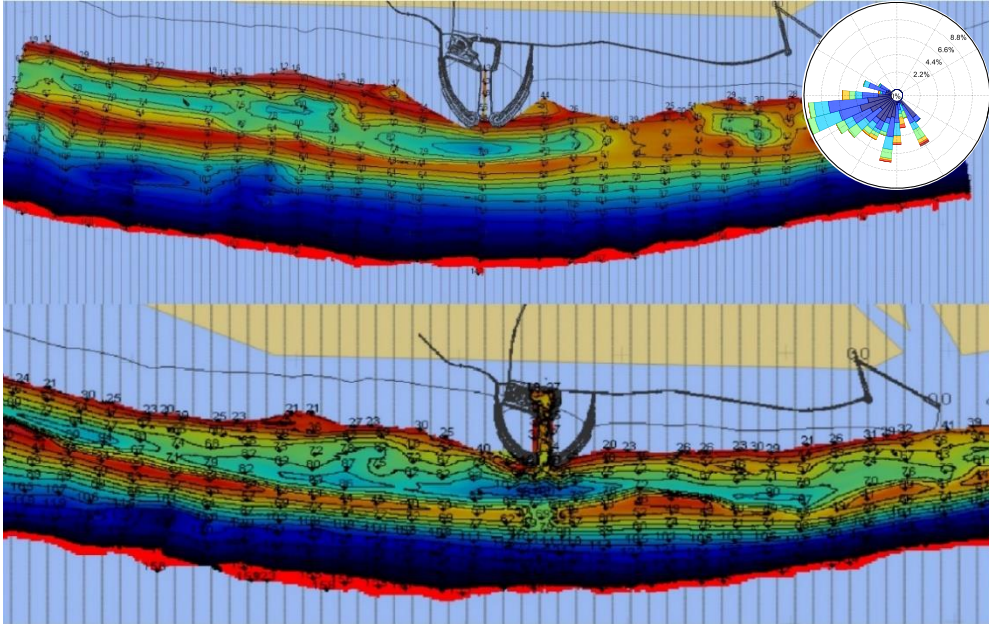


Figure 56: The measured bathymetries on the 18th of January 2015 and 7th of May 2015.

Small trends can be observed in the movement of the bar due to the prevailing wave climate. Large waves propagating predominantly from southeast form a westward sediment transport, which give rise to a westward movement of the bar. Wave propagating from the southwest generate an eastward sediment transport, which gives rise to an eastward movement of the bar. For larger figures of the five wave roses, see Appendix 15.2.

9.2 Bar Evolution and Comparison

From the Cascade simulations, the bar volume was obtained at selected locations. The evolution of the bar volume is calculated based on the cross-shore sediment transport, as briefly outlined before. Figure 57 shows the simulated variation in the bar volume at the harbour, from the 1st of January 2011 to 7th of December 2015. The dots in the figure are the calculated bar volumes from the profile measurements during the same time period. In the figure the seasonal variation in the bar volume can be seen, with larger values in March to April and smaller in October to November. The observed bar volumes agree rather well with the calculated values, demonstrating the reliability of the model. Both east and west of the harbour seasonal variations in the bar volume can be observed, see Appendix 15.3.

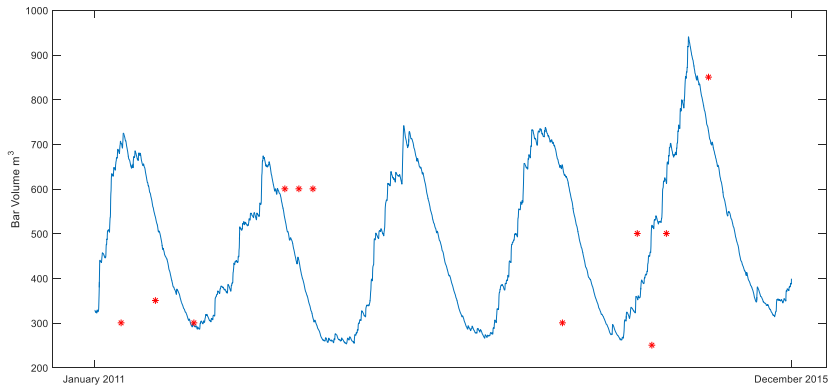


Figure 57: Calculated and measured bar volumes at the harbour from January 2011 to December 2015.

10 Analysis of Possible Solutions

This chapter presents a discussion of two possible solutions to the sedimentation problems that show greatest promise. The solutions are to construct groins or reservoirs, both with the aim to reduce the sediment transport to the harbour. Thus, lowering this transport is assumed to decrease the sedimentation around the entrance and to improve navigation conditions. Here, Cascade is used to model the groin solution, which includes periodic dredging. Reservoirs were investigated by Grunnet and Kristensen (2013), which is briefly described in 4.3.4; however, more studies were found to be needed regarding this solution. Since Cascade is not suitable for simulating the effects of reservoirs, the model was not employed to study this solution. The simulations for the groin solution were performed for a 10-year period (2005-2015).

10.1 Groins

The aim of placing groins at the location of the harbour is to trap sediment and reduce the transport to zero at the location of the harbour, thereby reducing the possibility of sediment accumulating in the entrance to the harbour. The groins should be long enough to reach the bar, since most of the LST occurs landward of the bar, which is located around 800 m from the shoreline. The groin solution was modelled with one groin placed on each side of the harbour, 400 m from the harbour, both with a length of 800 m.

Dredging operations may be needed when placing groins in coastal areas that trap excessive amount of sediment. The amount of sediment needed to be dredged is determined by the shoreline advance at the groin.

10.1.1 Results Groins

The model simulations show that minimal sediment is transported passed the groins initially. The area between the groins, where the harbour is located, are not analysed, since negligible amounts of sediment is transported into this area with little effects on the harbour. However, the results show that groins themselves will not be a sustainable solution due to the sediment trapping at the groins, which gives rise to a seawards migration of the shoreline and increased bypassing. Therefore, a combination of groins and periodic dredging operations are needed to achieve a sustainable solution.

For the groin 400 m east of the harbour, the shoreline is migrating seawards on the east side of the groin, see Figure 58. The amount required to be dredged to achieve a stable shoreline is about 40,000 m³/year. Figure 59 shows the shoreline variation east of the groin when dredging at 40,000 m³/year is performed, yielding a long-term stable shoreline.

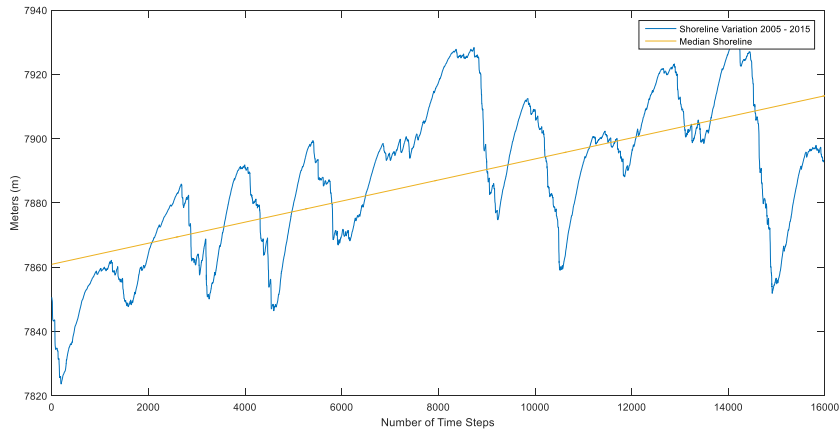


Figure 58: Shoreline evolution at the groin 400 m east of the harbour between 2005 and 2015.

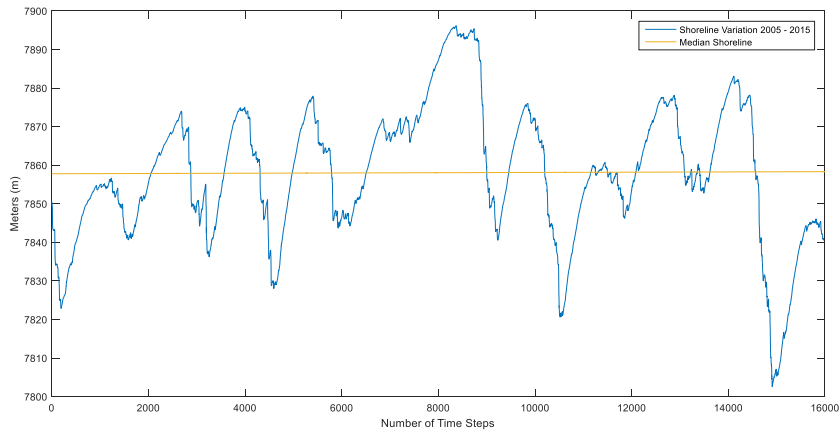


Figure 59: Shoreline evolution at the groin 400 m east of the harbour after continuous dredging between 2005 and 2015.

At the groin 400 m west of the harbour, the shoreline is migrating seawards on the west side of the groin, see Figure 60. The amount required to be dredged here to achieve a stable shoreline is about 125,000 m³/year. Figure

61 shows the shoreline variation west of the groin when a dredging operation of 125,000 m³/year is performed, yielding a stable shoreline.

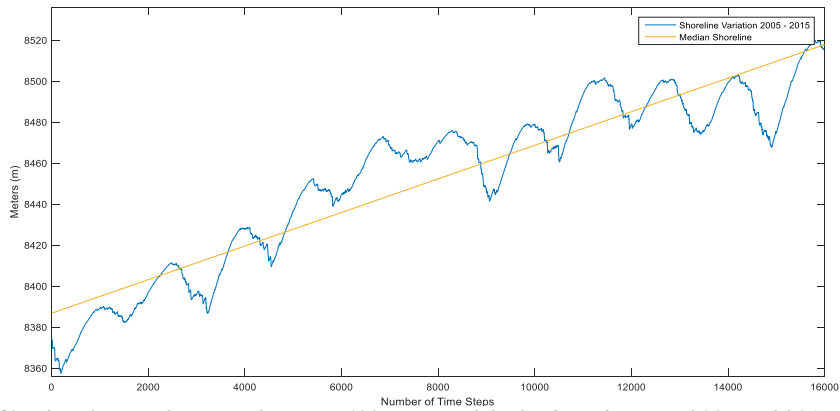


Figure 60: Shoreline evolution at the groin 400 m west of the harbour between 2005 and 2015.

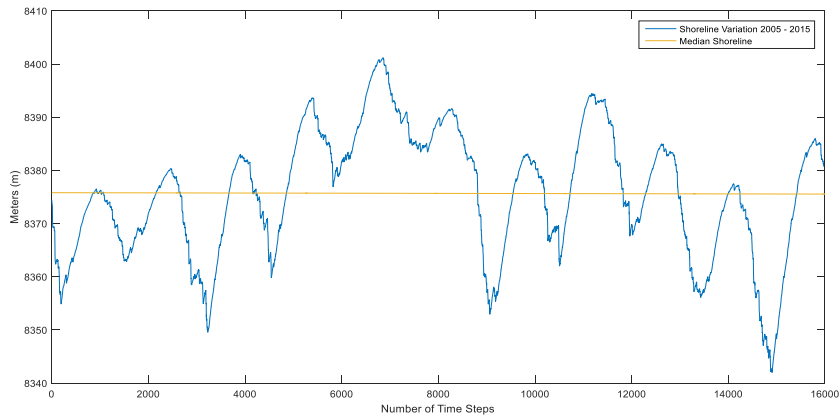


Figure 61: Shoreline evolution at the groin 400 m west of the harbour after continuous dredging between 2005 and 2015.

10.2 Reservoirs

The aim of placing reservoirs on both sides of the harbour is to trap sand in the reservoirs to reduce the sediment transport towards the harbour. This solution was discussed by Grunnet, Kristensen (2013), described in 4.3.4.4, which showed a trend to improve the sediment transport conditions.

Cascade that was used in this study does not resolve the cross-shore distribution of the LST. Therefore, the amount of sediment transported at the

bar and shoreline cannot be determined, which makes it difficult to model the effects of the reservoirs with Cascade. Thus, this solution was not modelled.

11 Discussion

This chapter discusses the LST models, the morphological evolution with focus on the bar, and the possible solutions investigated. The discussion focuses on evaluating model simulations and possible solutions, but also trends in the bar behaviour are reviewed.

11.1 Sediment Transport Modelling

The models, Qtrans and Cascade, which both simulated the LST at Landeyjahöfn yielded similar overall transport patterns. The Qtrans model provided a regional overview of the LST pattern, since the model is coarser in its spatial resolution with larger sections of the shoreline studied, whereas Cascade gave a more detailed picture due to the finer grid employed. The models predicted a LST pattern that fits relatively well with the shoreline evolution observed, although some differences occurred in the area east of the harbour. The sediment transport in this area is hard to determine since the area is complex with sediment supply from the river to the coast.

It is interesting to note that both models show a westward transport at the section of the harbour and a eastward transport west of the harbour, which indicates accumulation in this section. This result was not obtained in DHI modelling by Grunnet and Kristensen (2013), where only eastward net sediment transport could be observed over the profiles in this area. However, model simulations by DHI indicated a lowering of the westward sediment transport component over the area of the harbour (profile 0A and 0B), which should result in accumulation of sediment at the harbour. Accumulation at the harbour could be observed in the shoreline evolution, which displayed a seaward migration. The westward sediment transport at the section of the harbour obtained in the present study is primarily caused by the sheltering effect from the islands, since the waves propagating from the southwest are significantly reduced.

Another reason why the model simulation results in this study differ from DHI's could be the boundary conditions employed in the wave transformation model. The wave input in the EBED model used in this study was set only on the offshore boundary from one station when simulating the nearshore wave climates. In the corresponding simulations, DHI used

different input station at the boundaries. It is difficult to assess the impact of the different input conditions when simulating the wave climate without comparison with measured nearshore waves. However, in both Qtrans and Cascade the shoreline evolution has been taken into consideration when calibrating the sediment transport to match the evolution of the shoreline.

The simulations with the wave model EBED show that significant wave energy may enter the study area from the southeast. In the DHI simulations, waves propagating from southeast cannot be observed to the same extent. Movement of the bar towards the west has been recorded in the bathymetric surveys, indicating that the LST has been towards the west during certain periods. Therefore, it seems like Grunnet and Kristensen's (2013) modelling underestimated the waves propagating from the southeast, thereby estimating a LST towards the west that is too small.

11.2 Morphological Evaluation

Cascade modelled the bar evolution in terms of the variation in volume, where the observed trend from profile measurements was reproduced. To be able to validate short-term responses in the bar behaviour (e.g., storms), more detailed measurements of the profiles are needed, although it is believed that Cascade can model these responses reasonably well. Available measurements indicate that the bar is moving back and forth over time, but it is still rather stable in its mean position that points towards some sort of equilibrium between the incoming wave energy and the shoreline location.

11.3 Possible Solutions

Groins

The effect of the groin lengths should be investigated in more detail; if shorter groins would be able to decrease the sediment transport sufficiently at the harbour. However, to be able to evaluate the length of the groins a more refined description than what is employed in Cascade is needed that resolves the shape of the bar (in Cascade an equilibrium beach profile is used to calculate the bypassing ratio). If most of the sediment is transported close to the bar, then the length of the groins should most likely reach past the bar. On the other hand, if the sediment is mostly transported close to the shoreline then shorter groins could be a solution. Observations on the shoreline movement show that no up clear build-up of sediment has been observed

where the breakwaters were placed (Sigurdarson, 2016). This indicates that most of the LST occurs at the bar and therefore longer breakwaters are needed.

Since Cascade does not resolve the cross-shore distribution of the LST it is not possible to evaluate if shorter groins could be a viable solution. The groin lengths modelled in this study show that the LST will be completely blocked from entering the area between the groins, implying that this could be a solution to decrease the sedimentation at the harbour. If this is an acceptable solution, however, is mainly an economic decision. It is important to keep in mind that it is difficult to determine the detailed impact that the groins will have on the surrounding area based on the present modelling. What will happen in the area between the groins is difficult to say, although a more complex model may provide some answers. Since minimal sediment is transported to the area by LST, it is probable that the sedimentation problems in the harbour area will be reduced.

Reservoirs

If the purpose of constructing reservoirs is to achieve a long-term solution that will change the sediment equilibrium for the area, it will probably be very difficult. This is because the forces acting on the shoreline transporting sediment are mainly related to the shoreline orientation. Thus, the shoreline orientation has to be modified to change the conditions for the LST, which is both difficult and most likely not sustainable without a large-scale alterations of the shoreline.

The reservoirs could be a solution, if dredging operations are performed periodically, since sediment will deposit in the reservoirs. It was not possible to simulate this solution with the Cascade model since the behaviour of the reservoirs depend on the cross-shore distribution of the LST, as mentioned above. Thus, if the sediment is mostly transported at the bar the reservoir will have a minor impact on the sediment transport. On the other hand, if the LST mostly occur close to the shoreline the reservoirs will affect the sediment transport. For the reservoirs to trap sand a structure has to block or stop the sediment, which the harbour could achieve. However, when observing the shoreline after the placement of the breakwaters, no up build-up of sediment has been observed (Sigurdarson, 2016). This indicates that sediment is mostly transported at the bar, which implies that reservoirs would not be an efficient

solution to reduce the sediment transport. It also means that the breakwaters are not efficient in blocking sediment, which they were not supposed to be since they were constructed to achieve a bypassing effect. Therefore, reservoirs as a solution could be questioned.

12 Conclusions

The Landeyjahöfn harbour is exposed to sediment settling inside the harbour and at the entrance, which cause navigational problems for the ferry operating between the main land and the Westman Islands. A permanent solution for the siltation problems at the harbour is difficult to obtain, due to the complexity of the area and the large waves prevailing. The rough wave climate and orientation of the shoreline cause large LST rates along the shoreline passing the harbour at Landeyjahöfn, which leads to sediment entrainment and deposition at the harbour.

A 58-year long hindcasted offshore wave time series was employed to simulate the nearshore wave climate with the wave transformation model EBED. The simulation results showed, as expected, that the main nearshore waves at the study area were propagating from the southwest, but also a high proportion of waves could arrive from the southeast. At the location of the harbour the waves were mostly propagating from the southeast due to the sheltering effects from the Westman Islands. The sheltering effects can also be seen in the other shoreline sections in the vicinity to the harbour.

The models to calculate the LST rate, Qtrans and Cascade, indicated a dominant net transport to the east, in agreement with studies by DHI. However, in the coastal section at the harbour a distinct difference between the present models and the DHI model was observed. A westward LST was obtained in Qtrans and Cascade, as oppose to the DHI model that showed an eastward transport in this area. This westward transport is explained by the sheltering effect from the Westman Islands, which reduce the waves propagating from the southwest, thereby effecting the LST. This contributes to the accumulation in the area of the harbour, which could be a reason for the siltation problems. Also the magnitude of the LST was different, where the LST rates given by DHI were larger than for the two models employed in this study. In Cascade the shoreline evolution was also modelled, showing good agreement with measurements west of the harbour, which supported the model results in the present investigation. In the areas around the harbour, as well as further to the east, the shoreline evolution was more difficult to simulate with the model, depending on the sediment supply from the river and its shifting position together with the complex shoreline curvature.

The evaluation of the longshore bar evolution shows that the bar moves back and forth from east to west, due to the wave climate variations. The bar moves towards the east when waves are propagating from the southeast. Movement of the bar towards the west is observed when waves from the southeast are propagating towards the coast. Longshore movement of the bar is low during the summer compared to the winter due to the calmer wave climate during the former period. The volume of the bar has shown to vary also due to the annual variation of the wave climate and its effect on the cross-shore transport, where high bar volumes occur in March to April and low bar volumes in October to November. The comparison between the simulated bar volumes in Cascade and bar volumes derived from beach profile measurements indicated similar trends. Simulation results and measurements indicated that there is an equilibrium between the wave climate and shoreline position, both regarding the cross-shore and longshore transport. The mean position of the bar has been rather stable, even though its volume varies with time. More measurements of the beach profiles at finer temporal resolution are needed to clearly establish bar behaviour.

Groins reaching past the bar could be a solution to reduce the LST at the harbour; however, periodic dredging operations would have to be performed to make this solution sustainable. To evaluate if shorter groin lengths would work that did not extend beyond the bar, a more detailed description of the cross-shore LST distribution is needed of where the sediment is moving in the nearshore area; this type of description is not included in Cascade.

To use reservoirs as a solution seems difficult and it is not possible to evaluate the outcome with Cascade. Dredging operation would have to be performed to maintain the reservoirs so they can trap sediment. The efficiency of the reservoirs is difficult to determine and depends on the where sediment is transported in the nearshore zone. Further investigations are needed to evaluate if reservoirs are a possible solution.

13 Further Investigations

Because of the time limitation and the models employed in the present study, it was hard to perform all investigations that were desirable. Further measurements of the beach profiles would be of interest in order to investigate the evolution of the bar. Such measurements would make it possible to better evaluate the simulated bar volume change in Cascade and might provide improved knowledge of the bar evolution during storms.

To be able to evaluate the possible solutions for the harbour, more detailed data is needed of where and in what quantities the sediment is moving in the nearshore zone as well as proper models to simulate this.

14 References

- Baptista, P. et al., 2014. Beach morphology and shoreline evolution: Monitoring and modelling medium-term responses (portuguese NW coast studysite). *Coastal Engineering*, Issue 84, pp. 23-37.
- Bayram, A., Larson, M. & Hanson, H., 2007. A new formula for the total longshore sediment transport rate. *Coastal Engineering*, 7 June, pp. 700-710.
- Bogi, S., 2014. *Morgonbladid*. [Online] Available at: <http://www.mbl.is/frettir/myndasyrpa/2152/#52521> [Accessed 20 4 2016].
- Dally, W. R., Dean, R. G. & Dalrymple, R. A., 1985. Wave Height Variation Across Beaches or Arbitrary Profile. *Journal of Geophysical Research*, 20 November, pp. 11,917-11,927.
- Elfrink, B., Brøker, I. & Viggósson, G., 2006. *Bakkajfara Sediment Transport and Morphology - Phase 1*, s.l.: DHI.
- GoogleEarth, 2016. *Google Earth*. [Online] [Accessed 2016].
- Grunnet, N., 2012. *Bakkajfara Additional Morphology Modelling*, s.l.: DHI.
- Grunnet, N. & Kristensen, S., 2013. *Landeyjahöfn Further investigations*, s.l.: DHI.
- Hanson, H., 2015. *VVR040 - Coastal Hydraulics*. Lund: s.n.
- Hjelmager Jensen, J. et al., 2007. *Bakkajfara Sediment Transport and Morphology - Phase 2*, s.l.: DHI.
- Jónsdóttir, J. F., 2006. *Markarfljót, calculated discharge with the WaSiM-ETH watershed model*, s.l.: Orkustofnun.
- Larson, M., Hanson, H. & Hoan, L. X., 2010. *Direct formula to complete wave height and angle at incipient breaking*, s.l.: s.n.
- Larson, M., Hanson, H. & Kraus, N. C., 2002. *Simulation of Regional Longshore Sediment Transport and Coastal Evolution - The "Cascade" Model*. s.l., World Scientific Press.

Mase, H., 2001. Multi-Directional Random Wave Transformation Model Based on Energy Balance Equation. *Coastal Engineering Journal*, 43(4), pp. 317-337.

Nam, P. T. & Larson, M., 2010. Model of Nearshore Wave and Wave-Included Currents around a Detached Breakwater. *Journal of Waterway, Port, Coastal, and Ocean Engineering*, June, pp. 156-176.

Nam, P. T., Larson, M., Hanson, H. & Hoan, L. X., 2009. A Numerical Model of Nearshore Waves, Currents, and Sediment Transport. *Coastal Engineering*, May, 56(11-12), pp. 1084-1096.

NOAA, 2015. *National Ocean Service*. [Online] Available at: http://oceanservice.noaa.gov/education/tutorial_currents/03coastal2.html [Accessed 08 03 2016].

Palalane, J. & Larson, M., 2016. A long-term coastal evolution model with longshore and cross-shore processes. *Journal of Coastal Research*.

Sadabadi, S. A. H., 2011. *Modeling Wave, Currents, and Sediment Transport in Ystad Bay*, Lund University: s.n.

Sadabadi, S. A. H. & Larson, M., 2012. Numerical Modeling of Wave Transformation and Sediment in Ystad bay. *VATTEN - Journal of Water Management and Research*, Issue 68, pp. 161-167.

Seymour, R. J., 2005. CROSS-SHORE SEDIMENT TRANSPORT. *Encyclopedia of Coastal Science*, p. 352.

Sigurdarson, S., 2016. Reykjavik: s.n.

TVRL, M. L. & H. H., 2005. *Issues Related to Sediment Transport and Morphological Evolution in Connection with Possible Construction of a Harbor at Bakkafjara*, Lund: TVRL.

U.S. Army Corps of Engineers, 1984. *Shore Protection Manual*. Washington(D.C.): Corps of Engineers, Coastal Engineers Research Center.

Wang, P. & Kraus, N. C., 1999. Longshore Sediment Transport Rate Measured by Short-Term Impoundment. *Journal of Waterway, Port, Coastal and Ocean Engineering*, 125(3), pp. 118-126.

Viggósson, G., 2006. *Ferjuhöfn við Bakkafjöru - Áfangaskýrsla um rannsóknir og tillögur*, s.l.: Siglingastofnun.

15 Appendix

15.1 Shoreline Difference

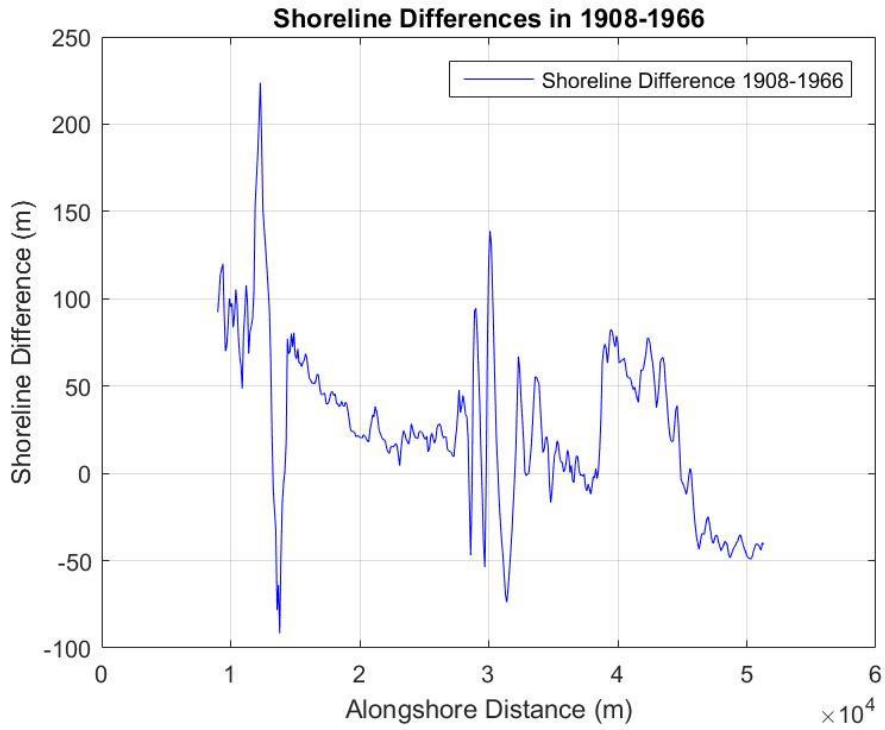


Figure 62: Shoreline difference between 1908-1966.

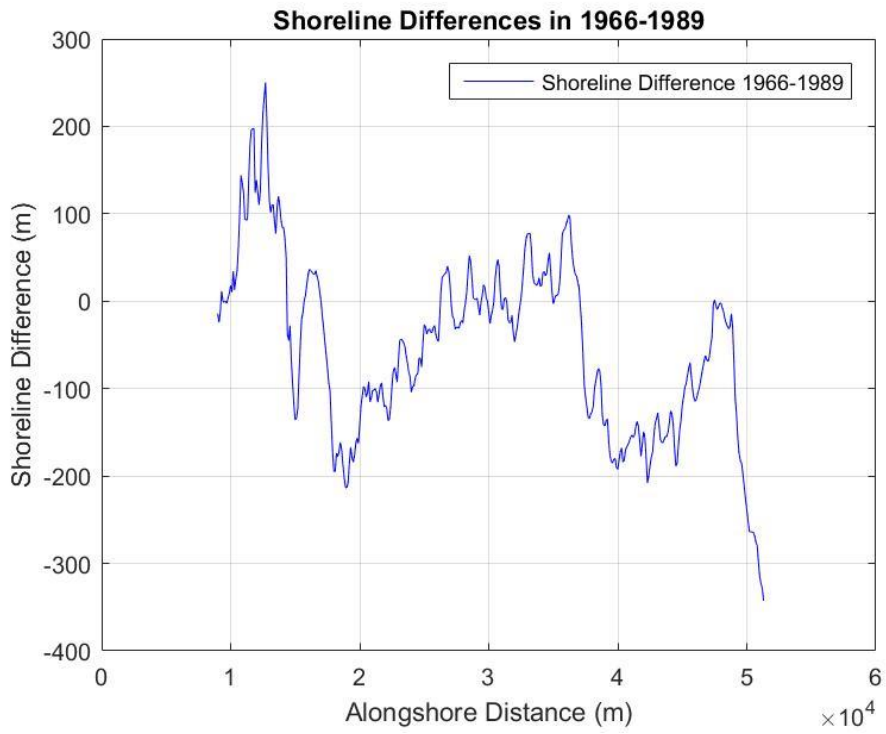


Figure 63: Shoreline difference between 1966-1989.

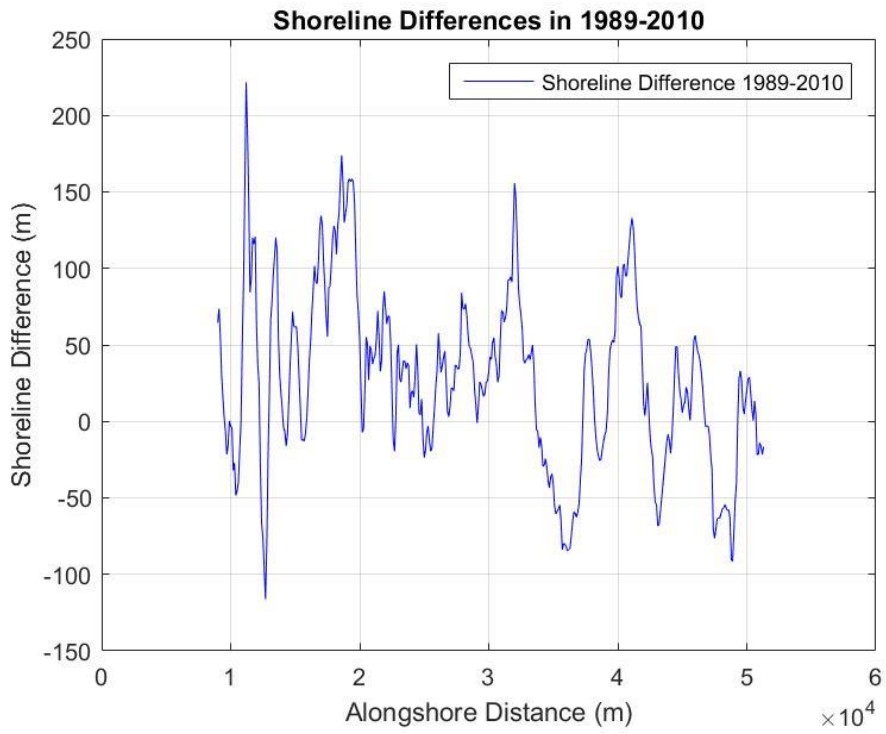


Figure 64: Shoreline difference between 1989-2010.

15.2 Wave Rose for Bar Evolution

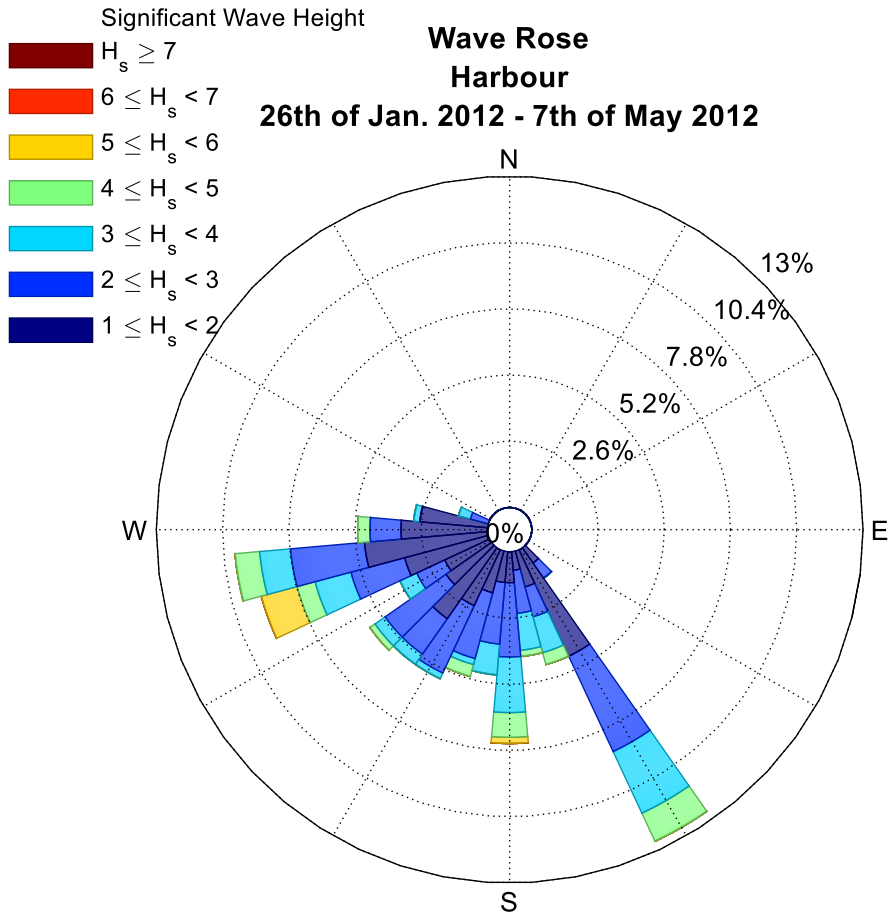


Figure 65: Wave rose of the wave climate at the harbour from 26th of Jan. 2012 to 7th of May 2012.

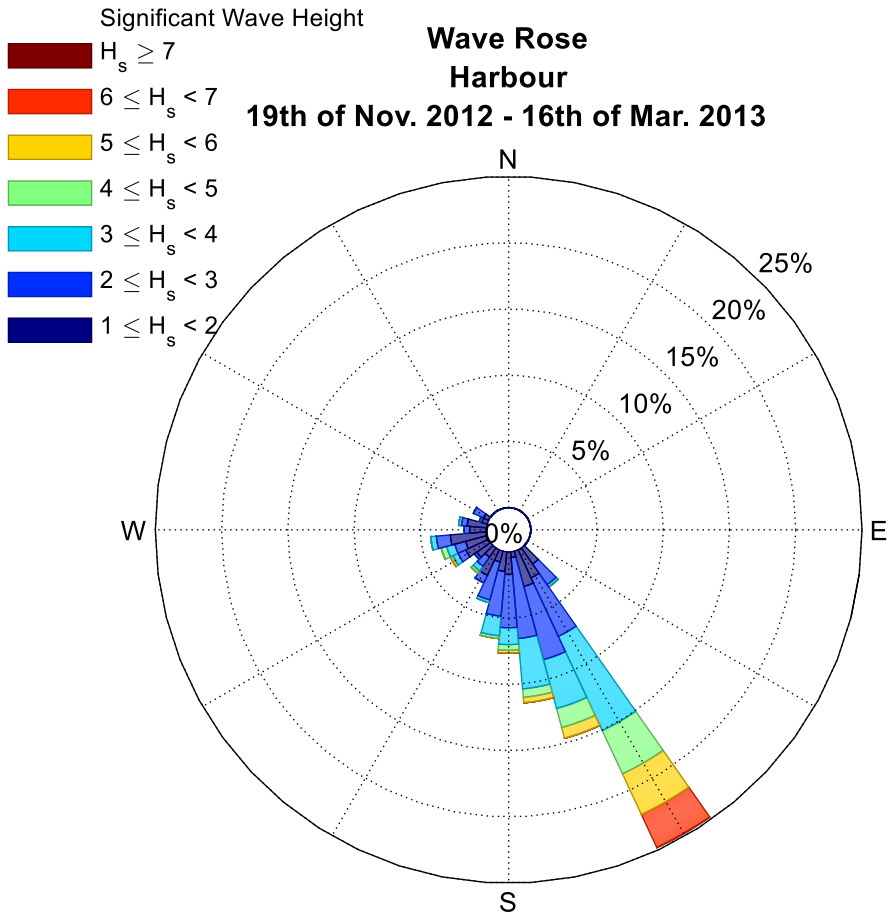


Figure 66: Wave rose of the wave climate at the harbour from 19th of Nov. 2012 to 16th of Mar. 2013.

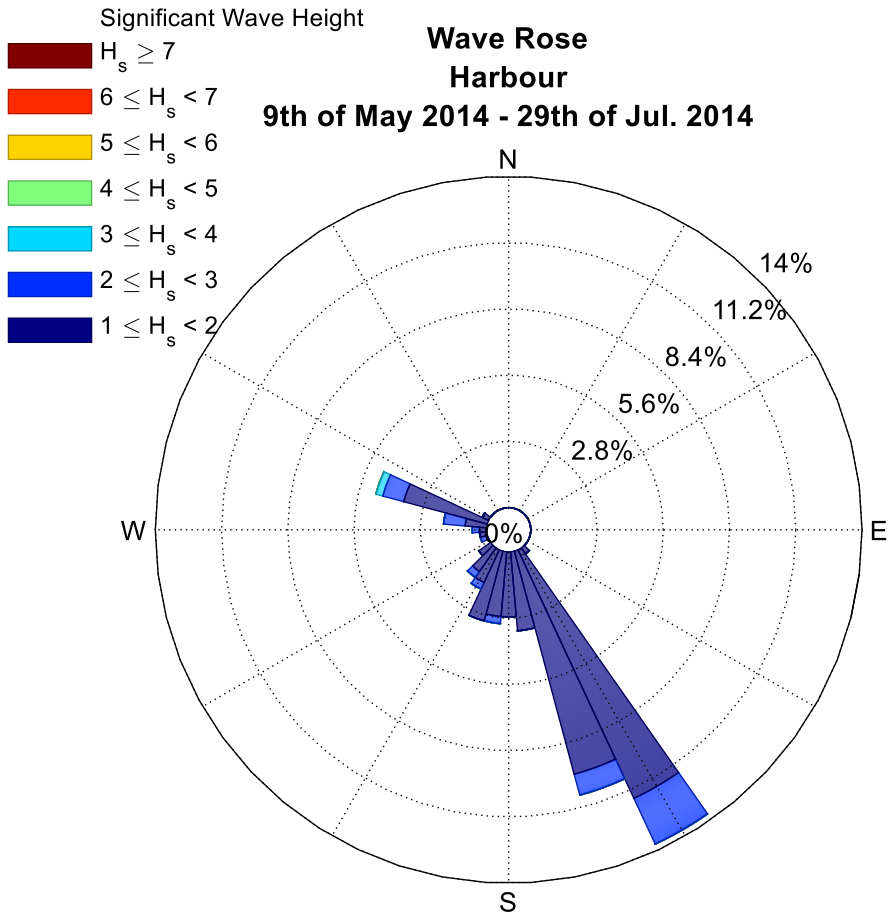


Figure 67: Wave rose of the wave climate at the harbour from 9th of May 2014 to 29th of Jul. 2014.

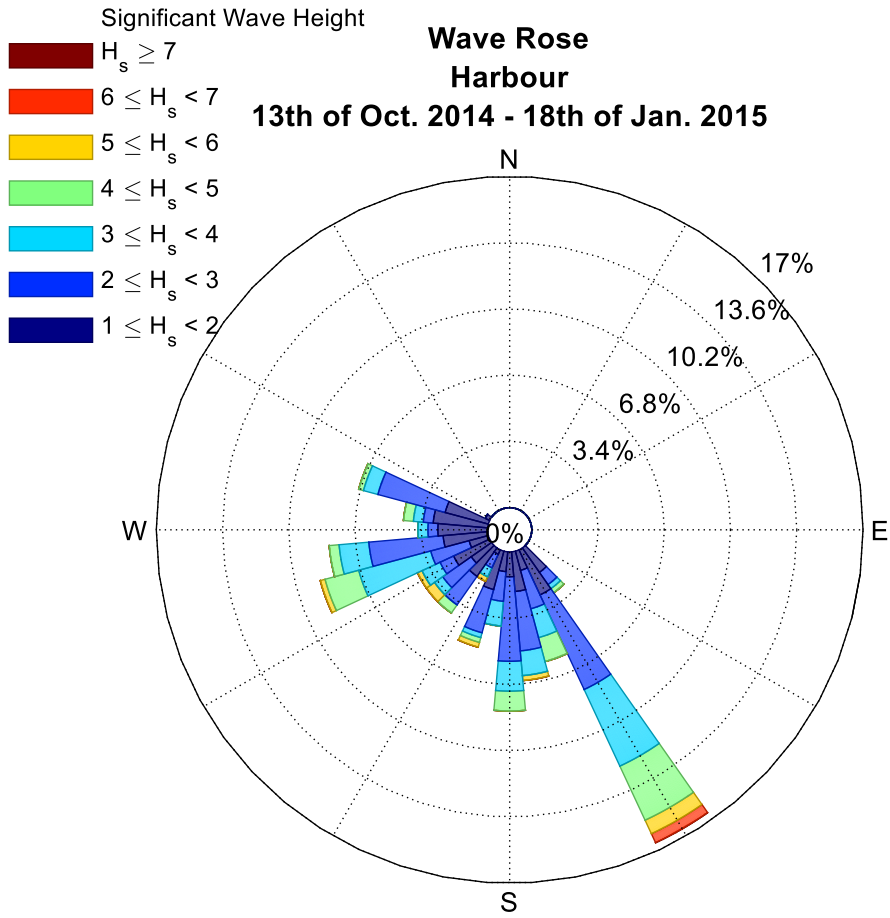


Figure 68: Wave rose of the wave climate at the harbour from 13th of Oct. 2014 to 18th of Jan. 2015.

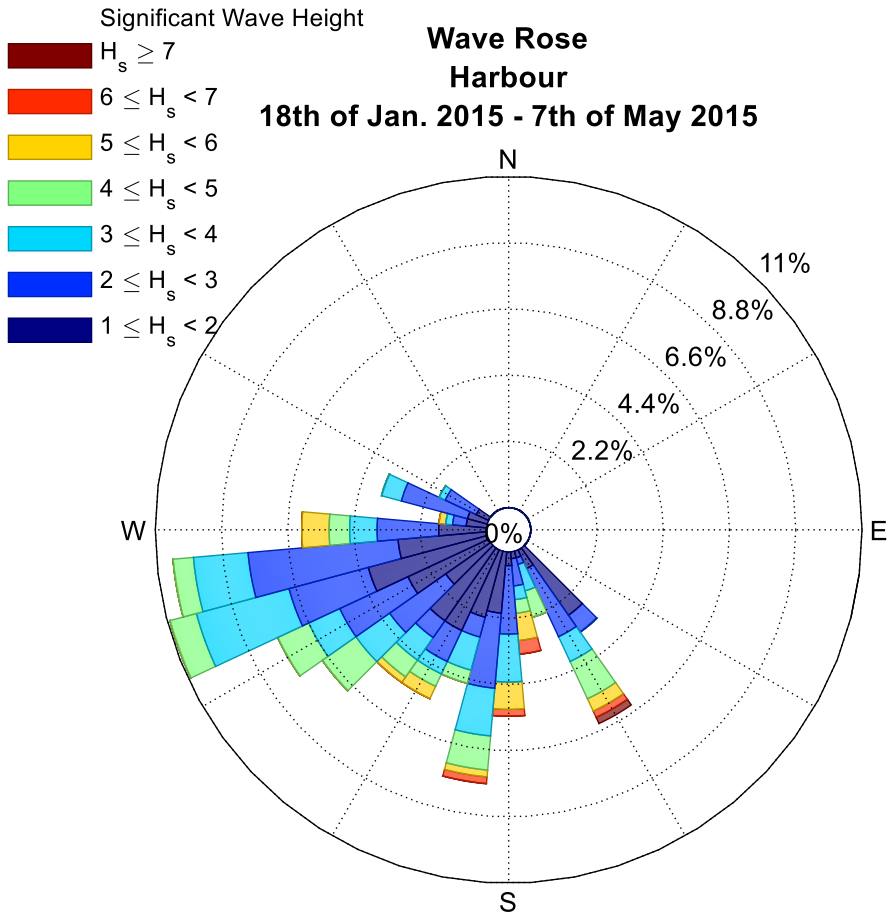


Figure 69: Wave rose of the wave climate at the harbour from 18th of Jan. 2015 to 7th of May 2015.

15.3 Bar Volume Variation

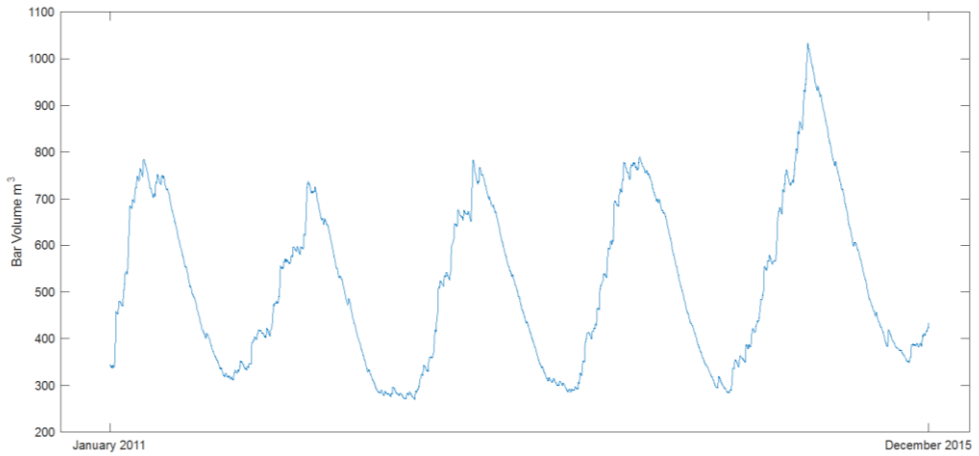


Figure 70: Bar volume 2011 - 2015 400 meters east of the harbour.

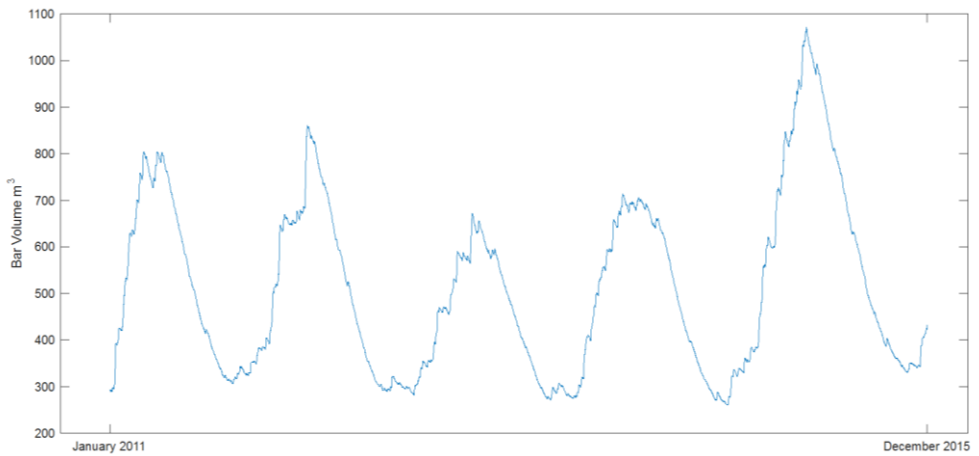


Figure 71: Bar volume 2011 - 2015 400 meters east of the harbour.